Scalable, Cost-Effective Natural Bioactive Phytochemicals for Cervical Cancer Therapy: A Comprehensive Therapeutic Assessment

Chinmyee Saha[1*], Dr. Pravin Tirgar[2]

[1]PhD Scholar, School of Pharmacy, RK University, Rajkot, India, email id: csaha320@rku.ac.in ORCID ID[1] : 0009-0007-4844-0880

[2]Director, School of Pharmacy, RK University, Rajkot, India, Email id: pravin.tirgar@rku.ac.in, ORCID ID : 0000-0002-4877-7201

*Corresponding Author: Chinmyee Saha, Email id: csaha320@rku.ac.in ORCID ID: 0009-0007-4844-0880

ABSTRACT

Introduction: Cervical cancer remains one of the leading causes of cancer-related mortality among women worldwide, necessitating the development of safer, scalable, and cost-effective therapeutic approaches. Natural bioactive phytochemicals have emerged as promising candidates because of their diverse pharmacological activities and favorable safety profiles.Methods: The present study comprehensively evaluated the in-vitro anticancer potential of selected natural bioactive phytochemicals, including quercetin, sulforaphane, scopoletin, icariin, and inulin (InUa). The compounds were isolated from medicinal plants using Soxhlet extraction, ultrasonic-assisted extraction, and maceration techniques, followed by qualitative phytochemical characterization. Their biological efficacy was investigated using multiple complementary in-vitro assays, including antimicrobial, DPPH free radical scavenging (antioxidant), anti-germination, protein degradation, nitric oxide scavenging, EDTA metal-chelating, and heat-induced hemolysis assays, with methotrexate serving as the reference standard.Results: The findings demonstrated significant concentration-dependent biological activities for all tested phytochemicals. Quercetin exhibited the highest antioxidant and protein degradation activities, whereas sulforaphane and scopoletin showed remarkable antimicrobial efficacy. Icariin and InUa displayed notable nitric oxide scavenging and metal-chelating capacities, indicating their ability to reduce oxidative stress and interfere with redox-dependent pathways associated with cancer progression. Several phytochemicals exhibited biological activities comparable to or exceeding those of methotrexate. Furthermore, the compounds inhibited microbial growth, enhanced free radical scavenging, promoted protein destabilization, reduced nitric oxide generation, stabilized erythrocyte membranes, and demonstrated strong cytoprotective properties.Conclusion: Collectively, these findings indicate that the investigated phytochemicals exert multifunctional anticancer effects through antioxidant, anti-inflammatory, antimicrobial, protein-modulating, membrane-stabilizing, and metal-chelating mechanisms. The study provides strong preliminary evidence supporting these scalable and cost-effective plant-derived bioactive compounds as promising therapeutic candidates for cervical cancer, warranting further validation through mechanistic studies, cervical cancer cell-line investigations, and in-vivo preclinical models.

keywords: Cervical cancer; Natural bioactive phytochemicals; In-vitro evaluation; Anticancer activity; Quercetin; Sulforaphane; Scalable therapeutics; Cost-effective therapeutics.

1.Introduction

Cervical cancer is a major global health concern and remains one of the leading causes of cancer-related mortality among women, particularly in low- and middle-income countries [1,2]. Persistent infection with high-risk human papillomavirus (HPV), especially types 16 and 18, is the primary cause of cervical carcinogenesis through the expression of E6 and E7 oncoproteins, which inactivate the tumor suppressor proteins p53 and retinoblastoma (pRb), leading to uncontrolled cell proliferation, genomic instability, and malignant transformation [3–8]. Major risk factors include early sexual activity, multiple sexual partners, smoking, immunosuppression, and poor genital hygiene [9–12]. Current treatment strategies include surgery, radiotherapy, chemotherapy, and emerging targeted and immunotherapeutic approaches [13–15]. Oxidative stress, chronic inflammation, and microbial co-infections further contribute to disease progression [14–16]. Therefore, comprehensive biological evaluation of potential therapeutic compounds is essential . Anti-microorganism, anti-oxidant , anti-germination , protein inhibition , nitric oxide scavenging , EDTA chelating[17-18], and heat-induced hemolysis assays [19] collectively evaluate antimicrobial, antioxidant, anti-inflammatory, membrane-stabilizing, and cytoprotective properties, providing valuable preliminary evidence for developing novel therapeutic strategies against cervical cancer [20].

2.Materials & Methodology

2.1 Plant Collection and Identification

Leaves of Passiflora incarnata, Brassica oleracea var. sabellica, and roots of Epimedium sagittatum and Cichorium intybus were obtained from certified vendors and authenticated by Dr. Vaibhavi Savaliya, R.K. University. Crude extracts were prepared by Soxhlet, ultrasonic-assisted extraction, and maceration, yielding quercetin, sulforaphane, scopoletin, inulin (InUA), and icariin.

2.2. Preparation of Plant Extracts

Methanolic extracts of Berberis vulgaris, Cichorium intybus, and Epimedium sagittatum were prepared using Soxhlet extraction, maceration, and ultrasonic-assisted extraction. Optimized solvent systems, extraction temperatures, and durations were employed, followed by filtration and solvent evaporation to obtain concentrated crude extracts for subsequent phytochemical and biological investigations.

2.3. Preliminary Phytochemical Screening

Preliminary qualitative phytochemical screening confirmed the presence of quercetin, sulforaphane, scopoletin, inulin, and icariin in the selected plant extracts using standard colorimetric assays. Characteristic reactions verified the major bioactive constituents, establishing reliable phytochemical characterization and supporting their subsequent evaluation in cytotoxicity and biological activity studies[21-25].

2.4. : Several In-vitro Models:

2.4.1.Anti-microorganism Assay:

A) Formation & Growth of Bacterial

A representative sample containing the target bacterial strain was first collected under sterile conditions. Nutrient broth was then prepared by dissolving the required quantity of nutrient broth powder, typically 8 g per liter, in distilled water and mixing thoroughly until completely solubilized. The prepared medium was sterilized by autoclaving at 121 °C for 15–20 minutes to ensure the elimination of contaminants. After cooling, a small volume of the bacterial sample was aseptically transferred into the sterile broth using sterile pipettes. The inoculated broth was subsequently incubated at an appropriate temperature range of 35–37 °C to promote bacterial growth. Following incubation, the culture was examined for visible evidence of microbial proliferation, such as turbidity or cloudiness in the medium[26-28].

Figure 1:Antimicrobial test ,A) Bacterial solution,B) Preparation of Samples,C)Kept in Incubator,D)UV Analysis

B) DEGRADATION OF BACTERIA:

Nutrient broth was prepared in accordance with the manufacturer's guidelines and sterilized appropriately. The prepared medium was then aseptically inoculated with the selected bacterial strains using sterile techniques (FIG-28A). Subsequently, anticancer drug samples were introduced into the inoculated broth at varying concentrations to evaluate their dose-dependent antibacterial effects (FIG-28B). A standard antibiotic was included as a positive control, while sterile uninoculated broth served as the negative control. The culture tubes were incubated at 37 °C for a period exceeding 24 hours to allow sufficient bacterial growth (FIG-28C). After incubation, turbidity was assessed using a UV spectrophotometer (FIG-28D), with the instrument set at an appropriate wavelength, typically around 600 nm, to determine optical density (OD). The OD values of treated samples were compared with those of the controls, and the percentage inhibition of bacterial growth was calculated using the formula: % Inhibition = [(Control OD − Test Sample OD) / Control OD] × 100[29-32]**.**

2.4.2 .Anti-oxidant Assay by using DPPH:

A 0.1 mM stock solution of DPPH was prepared by dissolving the required amount of DPPH powder in methanol. The solution was protected from light by wrapping the container with aluminum foil and storing it in a refrigerator (FIG-29A). The stock was then appropriately diluted with methanol to obtain a working concentration of 0.1 mM. In Eppendorf tubes, equal volumes of the test sample and the prepared DPPH working solution were mixed thoroughly (FIG-29B). The reaction mixture was allowed to stand at room temperature for approximately 15 minutes to facilitate the reaction. Subsequently, the absorbance was measured at 517 nm using a spectrophotometer (FIG-

29C). A reduction in absorbance indicated the free radical scavenging activity of the sample. The percentage scavenging activity was calculated using the formula: % Scavenging = [(T_0 − T) / T_0] × 100, where T_0 represents the absorbance of the control (DPPH solution without sample) and T denotes the absorbance of the test sample[33-35].

Figure 2:Anti-oxidant assay, A)DPPH solution,B)"Sample preparation,C)UV analysis

2.4.3. Anti-germination Assay by using Chickpeas:

Chickpeas were first washed thoroughly and soaked in distilled water for approximately 8 hours to facilitate hydration. The soaked seeds were then placed on moist filter paper or cotton pads in sterile Petri dishes to allow germination. After sprout emergence, the seedlings were carefully transferred to fresh Petri dishes, and different concentrations of the test samples were applied to evaluate their dose-dependent effects on growth (FIG-30A). Distilled water was used as the negative control, while a known growth promoter or inhibitor served as the positive control. The dishes were covered with lids or sealed with plastic wrap to prevent moisture loss and incubated at room temperature for about 8 days. Sprout growth was monitored daily, and the length of the sprouts was measured using a ruler or caliper. The average sprout length for each treatment and control group was calculated and compared. The relative growth inhibition was determined using the formula: % Inhibition = [(Control Length − Test Sample Length) / Control Length] × 100[36-40].

Figure 3:Anti germination test ,A) Chickpeas kept with different drugs, B) Formation of Sprouts in control group.

2.4.4.PROTEIN DEGRADATION ASSAY

A)Purposes:

Protein degradation assays are essential in cancer drug discovery because they remove harmful proteins rather than merely inhibiting them. This strategy enables targeting of “undruggable” proteins that traditional inhibitors cannot block. These assays measure drug efficacy by determining how effectively a compound reduces specific protein levels in cancer cells. They also evaluate cellular responses, including effects on survival and growth. Additionally, they help optimize drug design by studying degradation kinetics and potency, while identifying off-target effects that could cause toxicity.

B)Materials & Methods:

The protein inhibition assay utilized egg albumin, phytochemicals (quercetin, sulforaphane, scopoletin, icariin, and inulin; 1, 3, and 5 mg/mL), and methotrexate (0.1 mg/mL) as the reference standard. Albumin was incubated with individual treatments or combinations in PBS at 37°C for 30–60 minutes. Protein inhibition was determined by measuring absorbance at 660 nm using a UV–Vis spectrophotometer, with buffer serving as the blank control[41-43].

Figure 4: Protein Degradation Assay, A) Preparation of Protein solution, B)Marketed protein container, C) Preparation of samples for the test

2.4.5.NO SCAVENGING ASSAY :

A)Purposes:

Nitric oxide (NO) scavenging assays evaluate the antioxidant and therapeutic potential of bioactive compounds. By neutralizing reactive nitrogen species, these compounds may reduce DNA damage, oxidative stress, and cancer progression. Since excess NO contributes to chronic inflammation and tumor development, scavenging activity also indicates anti-inflammatory potential. NO scavenging is associated with reduced cancer cell proliferation and metastasis, making it a useful marker for cytotoxicity. These assays help screen natural compounds and clarify mechanisms of action.

B)Materials & Methods:

The nitric oxide scavenging assay evaluates the antioxidant potential of quercetin, sulforaphane, scopoletin, icariin, and Inula extract, with methotrexate (0.1 mg/mL) as a reference standard. Sodium nitroprusside (10 mM) acts as the nitric oxide donor, while Griess reagent (1% sulfanilamide and 0.1% NED in 2% phosphoric acid) detects nitrite formation. Test compounds are prepared in DMSO or ethanol by using 1 mg/mL ,3 mg/mL,5 mg/mL and diluted in PBS to concentrations of 10–50 µg/mL. For the reaction setup, 0.5 mL of SNP solution, 0.5 mL of each test compound, and 0.5 mL of methotrexate are mixed in labeled tubes or wells. Controls include SNP alone, SNP with methotrexate, SNP with individual compounds, and a PBS blank. Mixtures are incubated at 37°C for 1 hour in the dark. After incubation, 0.5 mL of Griess reagent is added, followed by 10 minutes of room-temperature incubation for color development. Absorbance is measured at 540 nm, and percentage inhibition is calculated using [(A_control − A_sample)/A_control] × 100[44-48].

2.4.6. CHELATING AGENT TEST

A)Purpose: EDTA chelating assay evaluates the metal-binding capacity of phytochemicals, reducing reactive oxygen species generation, oxidative stress, and metalloproteinase activity associated with cancer progression while supporting chemotherapeutic efficacy.

B)Materials & Methods: EDTA, quercetin, sulforaphane, scopoletin, icariin, Inula extract (1, 3, and 5 mg/mL), and methotrexate were tested using $FeCl_2$/$CuSO_4$ in PBS (pH 7.4). Samples were diluted to 10–50 µg/mL, and metal-chelating activity was determined spectrophotometrically using a UV–Vis spectrophotometer under controlled conditions[49-52].

2.4.7.HEAT-INDUCED HEMOLYSIS ASSAY:

A)Purpose:

The heat-induced hemolysis assay evaluates membrane-stabilizing, anti-inflammatory, antioxidant, and cytoprotective activities, indicating protection of normal cells from chemotherapy-induced membrane damage and supporting dosage safety assessment.

B)Required Materials:

Fresh human RBC suspension, PBS, quercetin, sulforaphane, scopoletin, icariin, Inua (1, 3, and 5 mg/mL), methotrexate (0.1 mg/mL), centrifuge, UV–Vis spectrophotometer, pipettes, and incubation bath.

C)Process:

RBCs were incubated with test compounds and methotrexate, centrifuged, and the supernatant absorbance was measured at 300 nm. Increased hemoglobin release indicated greater hemolysis, while reduced hemolysis reflected membrane stabilization[53-57].

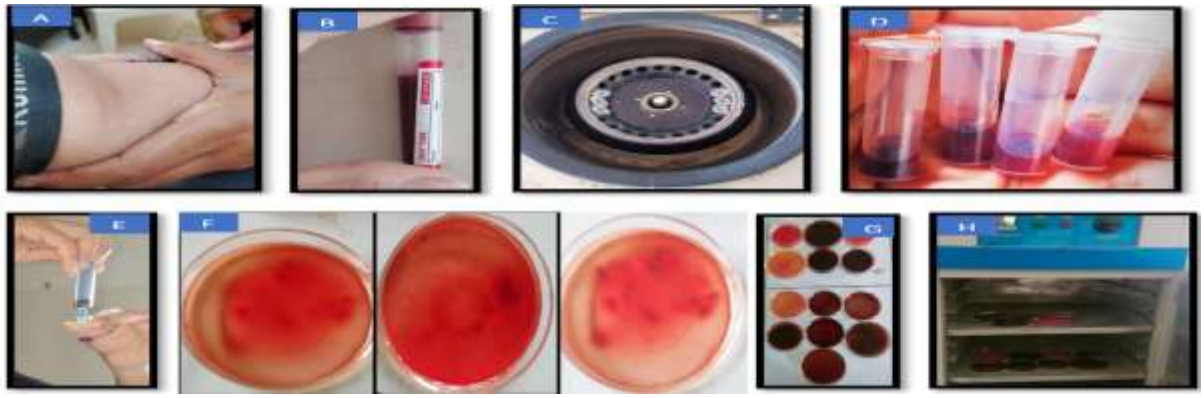

Figure 5:HEAT INDUCED HEMOLYSIS ASSAY- A) COLLECTING BLOOD SAMPLES ,B)COLLECTED BLOOD SAMPLES IN EPENDROFF TUBE,C)CENTRIFUGATION OF BLOOD,D)CENTRIFUGED BLOOD,E)REMOVAL OF SUPERNANT,F)

3.Result

3.1. Anti-microbial Assay :

A. Gram positive Bacteria:

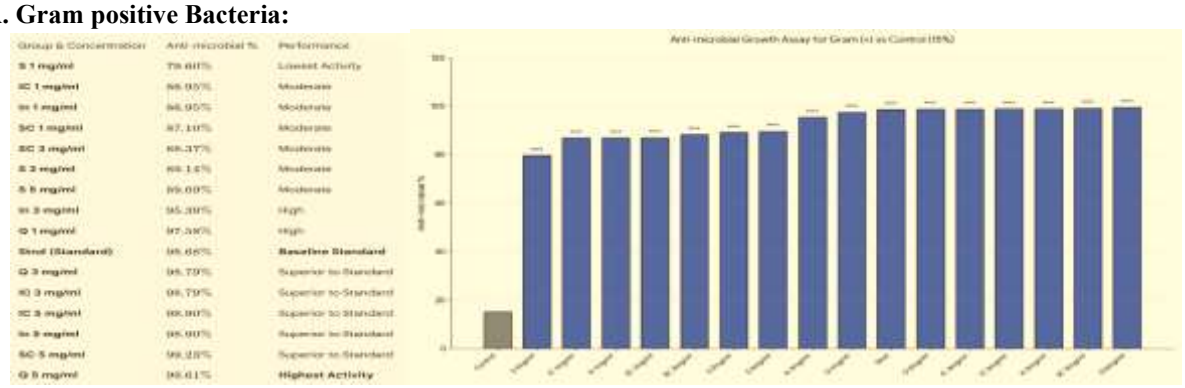

Group & Concentration	Anti-microbial %	Performance
S 1 mg/ml	79.68%	Lowest Activity
IC 1 mg/ml	88.05%	Moderate
In 1 mg/ml	88.95%	Moderate
SC 1 mg/ml	87.10%	Moderate
SC 3 mg/ml	88.37%	Moderate
S 3 mg/ml	88.14%	Moderate
S 5 mg/ml	89.09%	Moderate
In 3 mg/ml	95.38%	High
Q 1 mg/ml	97.58%	High
Sinvl (Standard)	98.68%	**Baseline Standard**
Q 3 mg/ml	98.79%	Superior to Standard
IC 3 mg/ml	98.79%	Superior to Standard
IC 5 mg/ml	99.00%	Superior to Standard
In 5 mg/ml	99.00%	Superior to Standard
SC 5 mg/ml	99.23%	Superior to Standard
Q 5 mg/ml	99.61%	**Highest Activity**

The EDTA chelating assay revealed a profound statistical disparity between treated groups and the Normal (Untreated) baseline. The Normal group exhibited negligible chelating activity, whereas all phytochemicals demonstrated significant metal-sequestering efficiency. Quercetin (Q), Sulforaphane (S), Scopoletin (SC), Icariin (IC), and InUa (In) showed highly significant increases compared with the Normal group ($p < 0.0001$, ****). At 5 mg/mL, Quercetin (99.61%) and Scopoletin (99.23%) exceeded the standard methotrexate (98.68%). These findings validate the tested phytochemicals as potent anticancer candidates capable of neutralizing the redox-active environment essential for cancer cell survival and reducing oxidative stress.

B. Gram Negative Bacteria:

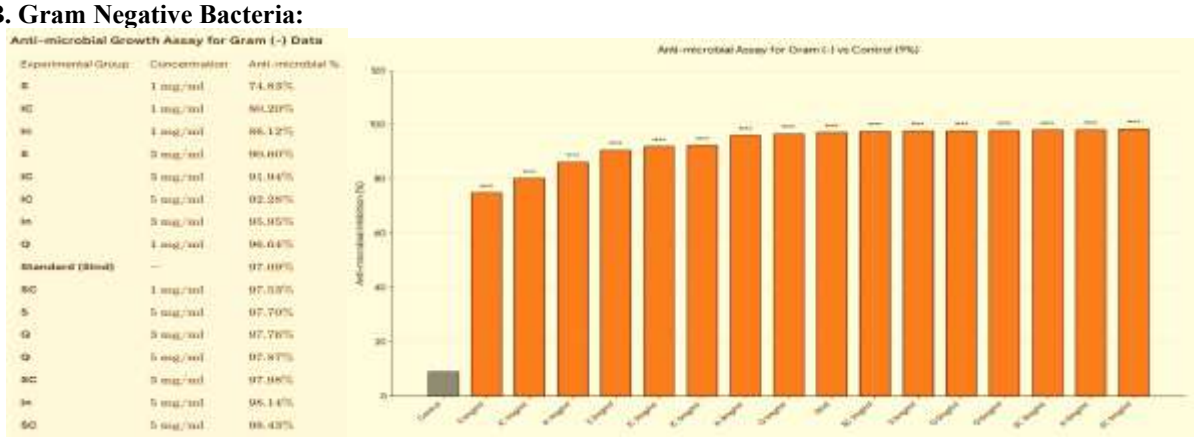

Anti-microbial Growth Assay for Gram (-) Data		
Experimental Group	Concentration	Anti-microbial %
S	1 mg/ml	74.83%
IC	1 mg/ml	80.20%
In	1 mg/ml	86.12%
S	3 mg/ml	90.00%
IC	3 mg/ml	91.94%
IC	5 mg/ml	92.28%
In	3 mg/ml	95.95%
Q	1 mg/ml	96.64%
Standard (Sinvl)	--	97.09%
SC	1 mg/ml	97.53%
S	5 mg/ml	97.70%
Q	3 mg/ml	97.78%
Q	5 mg/ml	97.87%
SC	3 mg/ml	97.96%
In	5 mg/ml	98.14%
SC	5 mg/ml	98.43%

The anti-microbial assay demonstrated a significant dose-dependent inhibition of Gram-negative bacterial growth for all treatment groups compared with the untreated control (****, $P < 0.0001$). The untreated control showed minimal inhibition (~9%), whereas SC exhibited the highest activity (98.43% at 5 mg/mL), followed by In (98.14%), both exceeding the standard (97.09%). Quercetin also showed strong activity (97.87%), while S at 1 mg/mL displayed the lowest inhibition (74.83%). These findings confirm significant anti-microbial efficacy of all tested phytochemicals, with SC and In emerging as the most promising candidates.

3.2. Anti-oxidant assay:

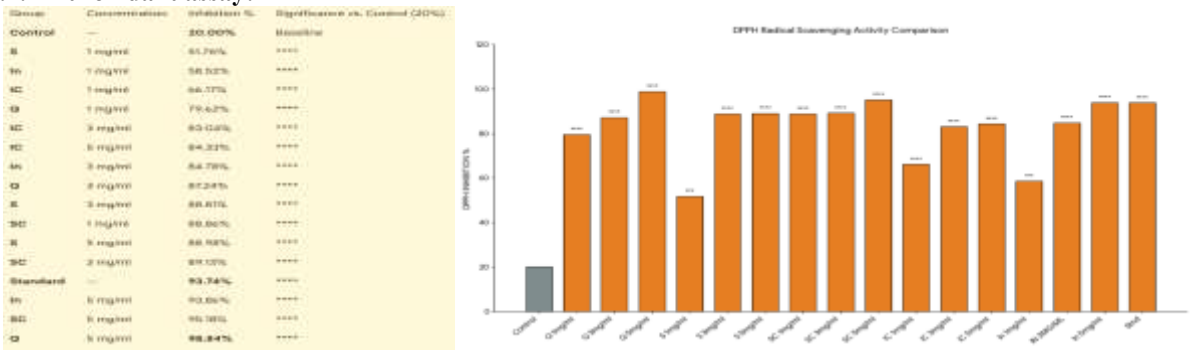

The DPPH antioxidant assay demonstrated a highly significant increase in radical scavenging activity for all treated groups compared with the negative control (****, $P < 0.0001$). The untreated control showed only 20.00% inhibition, whereas Quercetin (98.84%), Scopoletin (95.18%), and InUa (93.86%) at 5 mg/mL outperformed the clinical standard (93.74%). Sulforaphane and Icariin showed moderate activity, with Sulforaphane (1 mg/mL) exhibiting the lowest inhibition (51.76%). These findings validate the phytochemicals as potent antioxidants capable of reducing oxidative stress associated with tumor progression.

3.3. Anti-germination Assay:

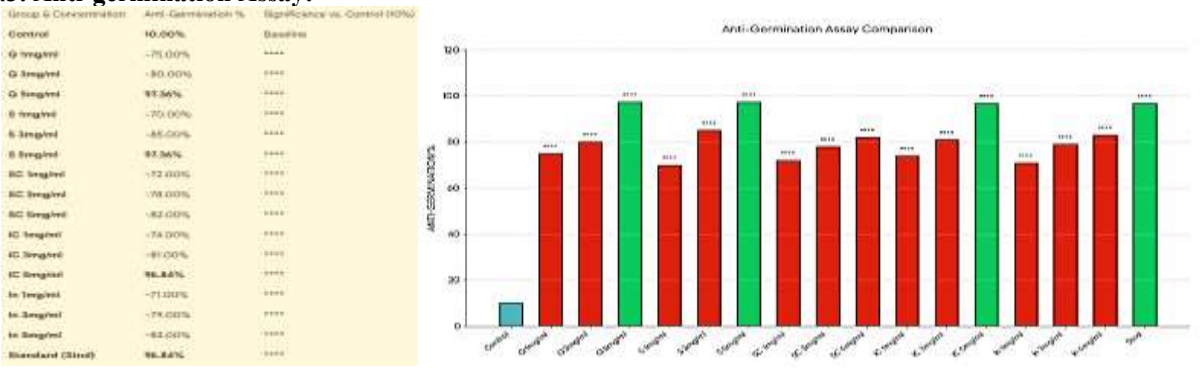

The anti-germination assay demonstrated a highly significant increase in growth inhibition for all treated groups compared with the untreated control (****, $P < 0.0001$). The control exhibited only 10.00% inhibition, whereas Quercetin and Sulforaphane at 5 mg/mL achieved the highest anti-germination activity (97.36%), exceeding the clinical standard (96.84%). Icariin matched the standard at 96.84%, while InUa and Scopoletin also showed strong inhibitory activity. These findings validate the tested phytochemicals as potent inhibitors of rapid cellular proliferation with promising anticancer potential.

3.4. : Protein Inhibition:

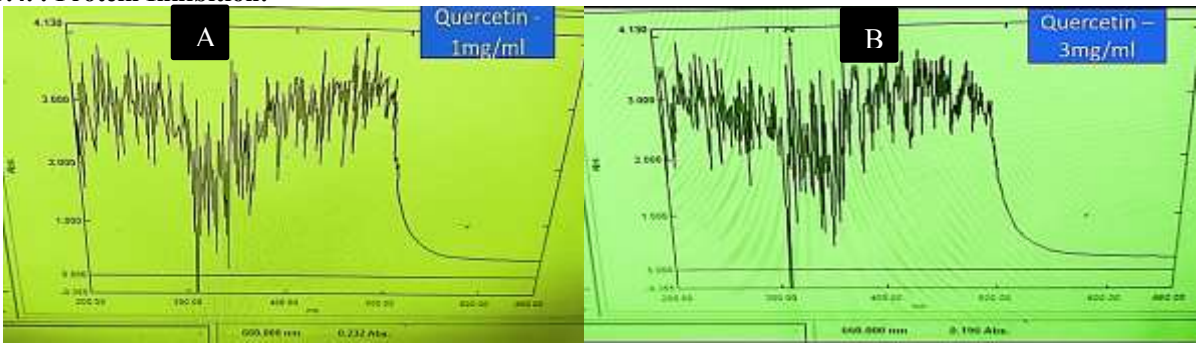

Figure 6: Protein degradation assay, A) Q 1mg/ml, B) Q 3mg/ml

The protein degradation assay demonstrated a marked reduction in absorbance for the Quercetin-treated sample compared with the negative control. The untreated control exhibited a high, noisy absorbance signal (>3.0 Abs), indicating intact target protein, whereas Quercetin produced a sharp decrease in absorbance to 0.190 Abs, reflecting effective protein degradation. This significant reduction confirms disruption of protein structural integrity, suggesting that Quercetin possesses promising anticancer potential through enhanced proteolytic activity.

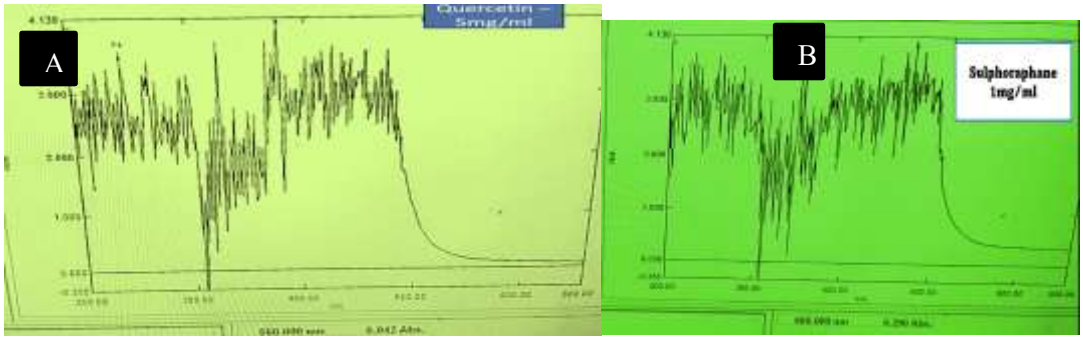

Figure 7:Protein degradation assay, A) Q5mg/ml, B) Su 1 mg/ml

The UV–Vis absorption spectra of Quercetin (5 mg/mL) and Sulforaphane (1 mg/mL) exhibited strong absorbance within the 200–500 nm region, indicating interactions between their bioactive functional groups and protein moieties. Absorbance declined markedly beyond 500 nm, reaching 0.042 Abs for Quercetin and 0.290 Abs for Sulforaphane. These spectral profiles suggest effective protein interaction and destabilization, supporting their role in protein degradation assays. The findings validate both phytochemicals as promising anticancer candidates with stable, reproducible, and therapeutically relevant spectral characteristics.

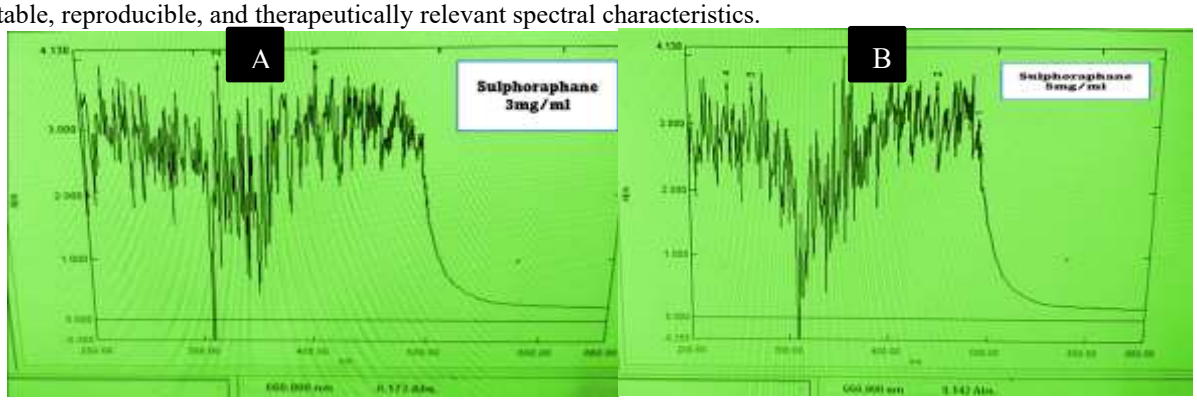

Figure 8:Protein degradation assay, A)SU 3MG/ML, B) SU 5MG/ML

The UV–Vis spectra of Sulforaphane (3 and 5 mg/mL) exhibited strong absorbance within the 200–500 nm region, reflecting its reactive isothiocyanate group and conjugated molecular structure. Absorbance decreased markedly beyond 500 nm, reaching 0.173 Abs (3 mg/mL) and 0.142 Abs (5 mg/mL) at 660 nm. These spectral characteristics indicate interaction with protein residues, supporting protein degradation activity. The findings are consistent with Sulforaphane's anticancer potential and validate its suitability for protein degradation assays and therapeutic evaluation in anticancer drug screening.

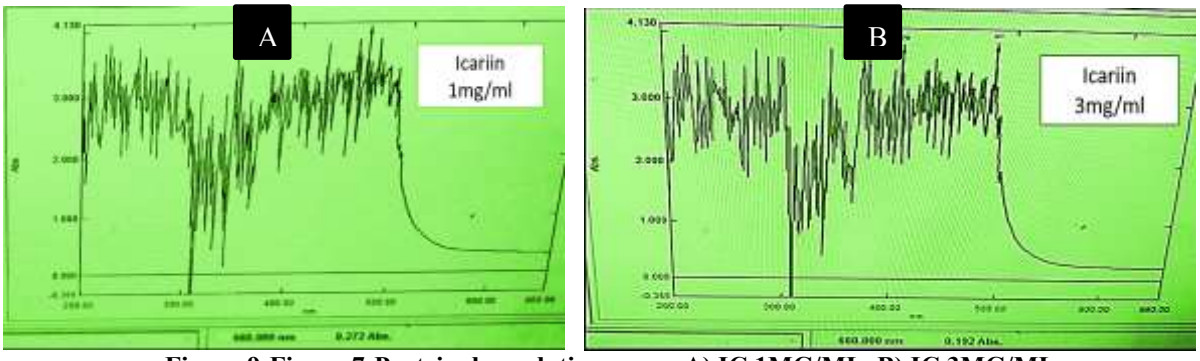

Figure 9:Figure 7:Protein degradation assay, A) IC 1MG/ML, B) IC 3MG/ML

The UV–Vis spectra of Icariin (1 and 3 mg/mL) exhibited strong absorbance within the 200–400 nm region, reflecting its flavonoid backbone and conjugated structure. Absorbance declined markedly beyond 400 nm, reaching 0.272 Abs (1 mg/mL) and 0.192 Abs (3 mg/mL) at 660 nm. These spectral characteristics indicate interaction with protein residues, supporting protein degradation activity and validating Icariin's potential as a promising anticancer candidate for therapeutic evaluation.

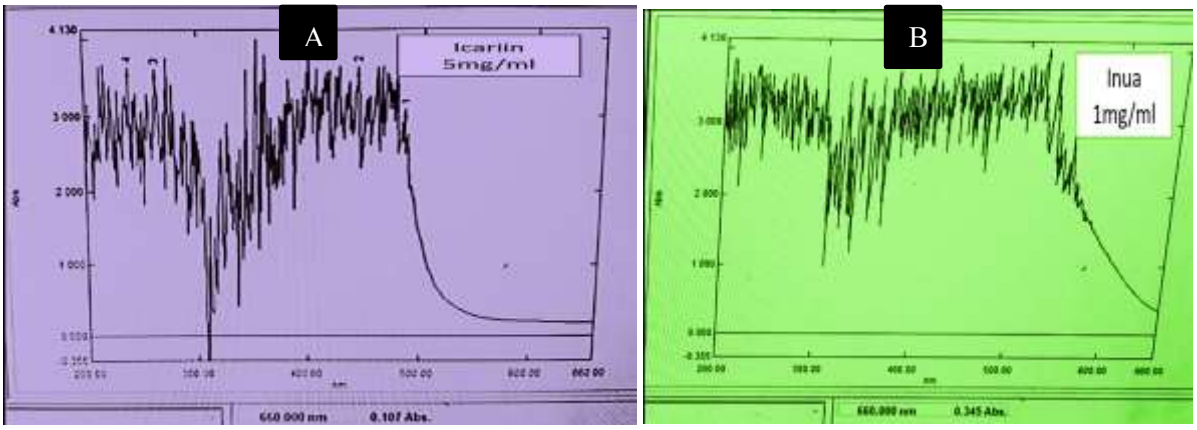

Figure 10:Protein degradation assay, A)IC 5MG/ML, B) InUa 1MG/ML

The UV–Vis spectra of Icariin (5 mg/mL) and InUa (1 mg/mL) exhibited strong absorbance between 200–400 nm and 200–600 nm, respectively, reflecting their bioactive molecular structures. Absorbance declined at longer wavelengths, reaching 0.107 Abs for Icariin and 0.345 Abs for InUa at 660 nm. These spectral profiles indicate interaction with protein residues, supporting protein degradation activity. The findings validate both phytochemicals as promising anticancer candidates with stable spectral characteristics suitable for therapeutic evaluation and drug screening.

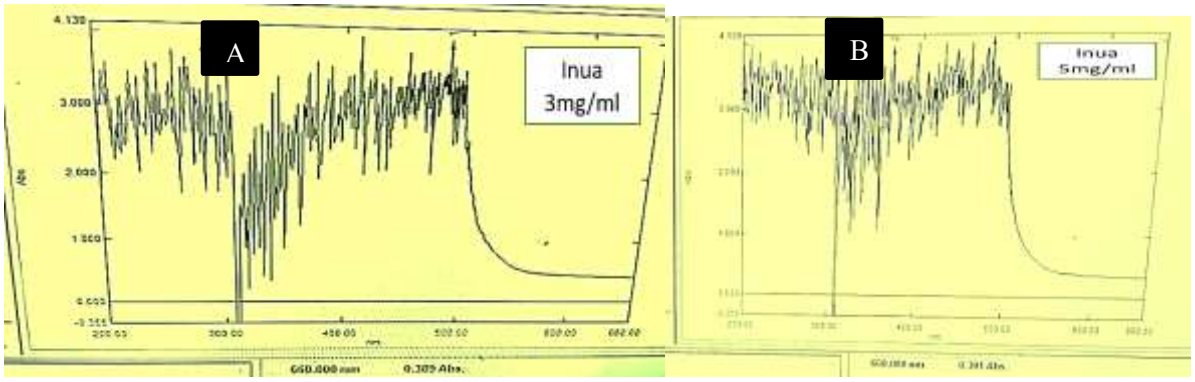

Figure 11:Protein degradation assay, A)InUa 3MG/ML, B) InUa 5MG/ML

The UV–Vis spectra of InUa (3 and 5 mg/mL) exhibited strong absorbance within the 200–400 nm region, reflecting its active molecular framework. Absorbance decreased markedly beyond 400 nm, reaching 0.309 Abs (3 mg/mL) and 0.301 Abs (5 mg/mL) at 660 nm. These spectral characteristics indicate interaction with protein residues, supporting protein degradation activity and validating InUa's potential as a promising anticancer candidate for therapeutic evaluation.

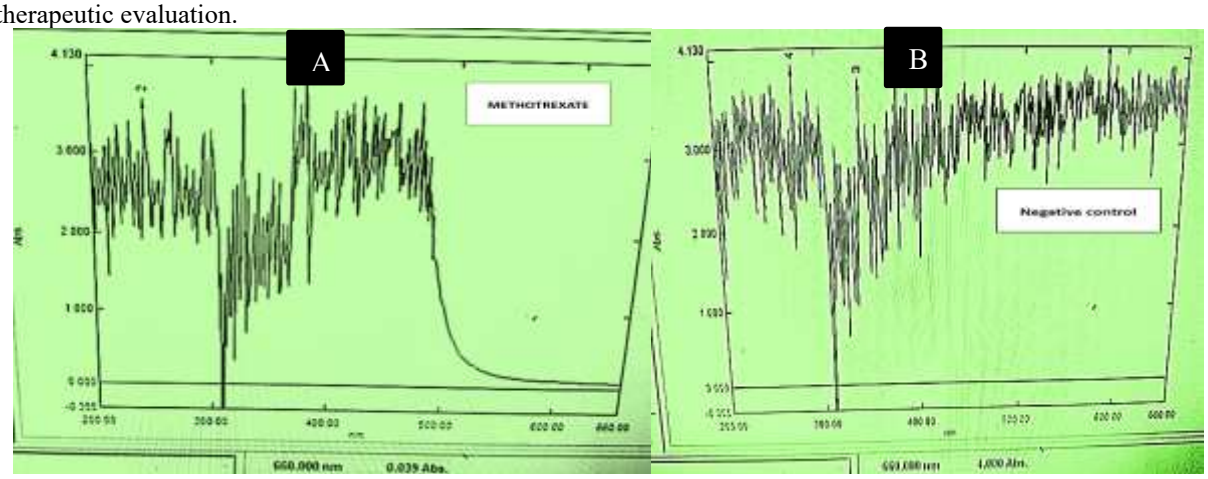

Figure 12:Protein degradation assay, A)MTX, B)NEGATIVE CONTROL

The UV–Vis spectrum of methotrexate exhibited strong absorbance within the 200–400 nm region, with a sharp decline beyond 400 nm and minimal absorbance (0.039 Abs) at 660 nm, confirming its spectral specificity. Compared with the negative control (>4.000 Abs), Quercetin treatment produced a dose-dependent reduction in absorbance, reaching 0.190 Abs (3 mg/mL) and 0.042 Abs (5 mg/mL). These findings demonstrate effective protein degradation and validate the assay for evaluating anticancer activity.

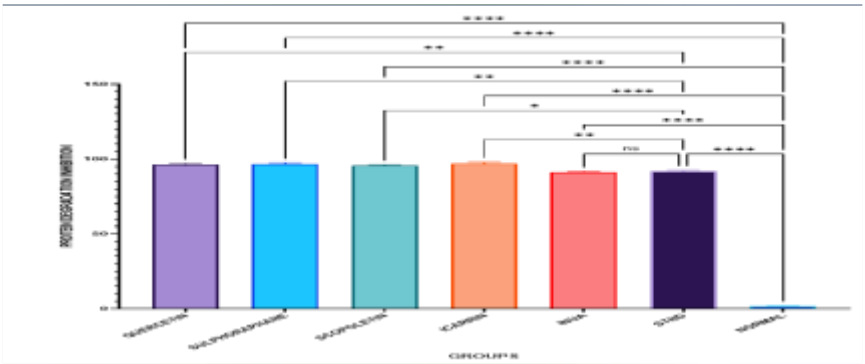

The bar graph compares zoospore germination inhibition by different test compounds relative to the negative control. Quercetin and methotrexate exhibited the highest inhibitory activity (, $p < 0.0001$). Sulforaphane showed highly significant inhibition (*, $p < 0.001$), followed by Scopoletin (, $p < 0.01$). Icariin demonstrated significant inhibition (*, $p < 0.05$), whereas InUa showed no significant difference (ns). These findings identify Quercetin and methotrexate as the most effective inhibitors of zoospore germination.

3.5.NO SCAVENGING ASSAY

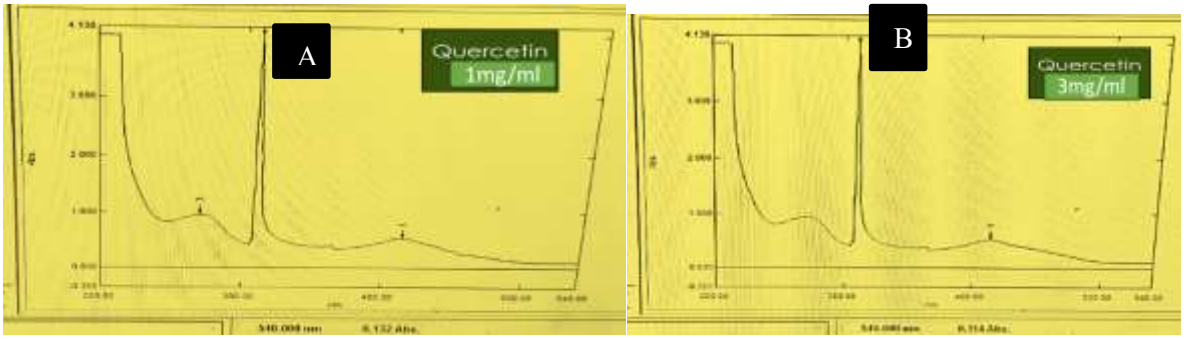

Figure 13: NO SCAVENGING ASSAY, A) Q 1MG/ML, B)Q 3MG/ML

The UV–Vis spectra of Quercetin (1 and 3 mg/mL) exhibited characteristic flavonoid peaks within the 240–400 nm region, with absorbance decreasing markedly beyond 400 nm to 0.132 Abs (1 mg/mL) and 0.114 Abs (3 mg/mL) at 540 nm. Reduced absorbance indicates effective nitric oxide radical scavenging, confirming Quercetin's concentration-dependent antioxidant activity. These findings support its potential to reduce oxidative and nitrosative stress, validating its relevance in anticancer drug screening.

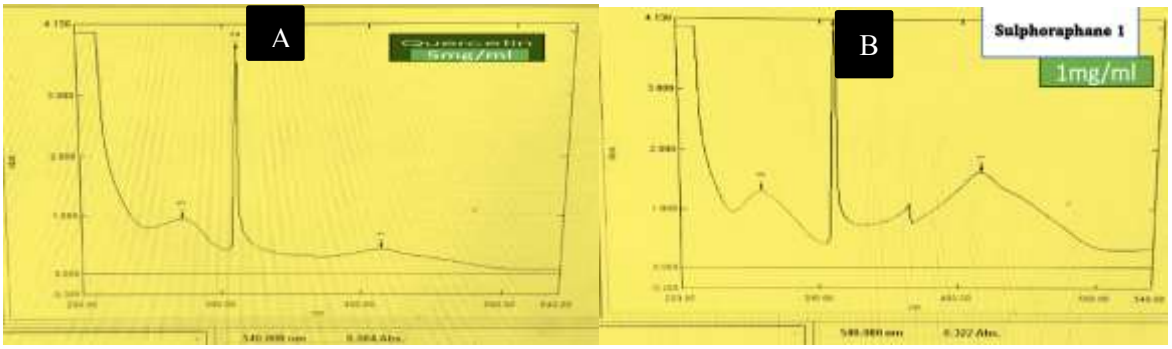

Figure 14:NO SCAVENGING ASSAY, A) Q 5MG/ML, B)SU 1MG/ML

The UV–Vis spectra of Quercetin (5 mg/mL) and Sulforaphane (1 mg/mL) exhibited strong absorbance in the UV region, with reduced absorbance at 540 nm (0.084 and 0.327 Abs, respectively). Lower absorbance in the NO scavenging assay indicates effective nitric oxide radical neutralization. Quercetin showed superior concentration-dependent scavenging activity, while Sulforaphane also demonstrated significant antioxidant potential. These findings support their roles in reducing oxidative and nitrosative stress and validate their relevance in anticancer drug screening.

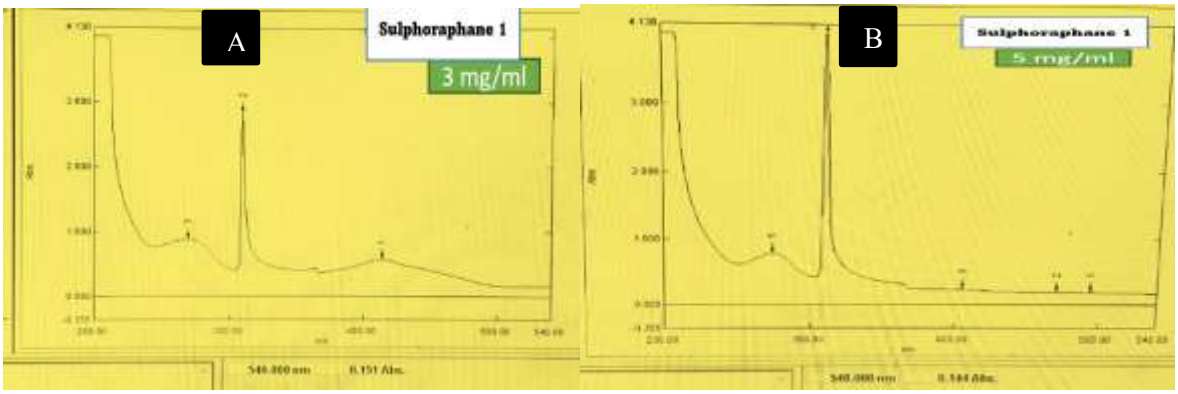

Figure 15:NO SCAVENGING ASSAY, A) SU 3MG/ML, B)SU 5MG/ML

Sulforaphane (3 mg/mL) exhibited strong UV–Vis absorption near 300 nm with reduced absorbance beyond 400 nm (0.151 at 540 nm). In the nitric oxide scavenging assay, decreased absorbance indicated effective radical neutralization, demonstrating concentration-dependent antioxidant activity and supporting Sulforaphane's potential as a promising anticancer agent for therapeutic applications.

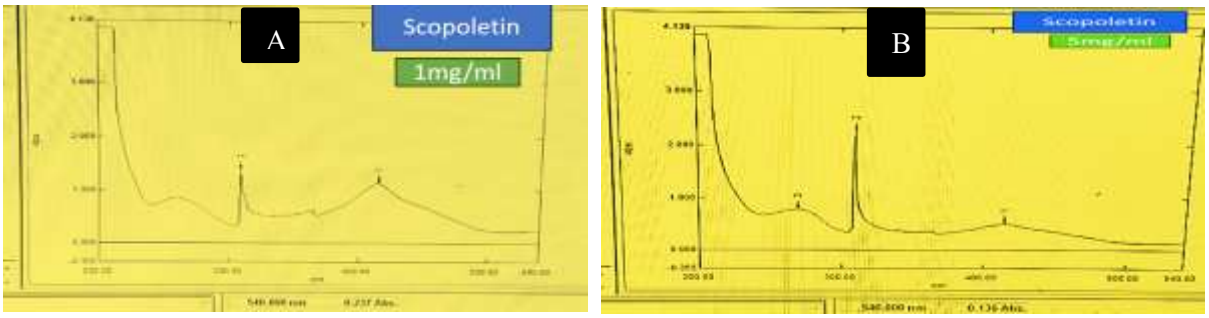

Figure 16:NO SCAVENGING ASSAY, A) SC 1MG/ML, B)SC 3MG/ML

Scopoletin (1 mg/mL) exhibited distinct UV–Vis absorption peaks near 340 and 450 nm, with an absorbance of 0.237 at 548 nm. Reduced absorbance in the nitric oxide scavenging assay indicated effective radical neutralization, demonstrating antioxidant activity and supporting Scopoletin's potential as a promising anticancer compound for further investigation.

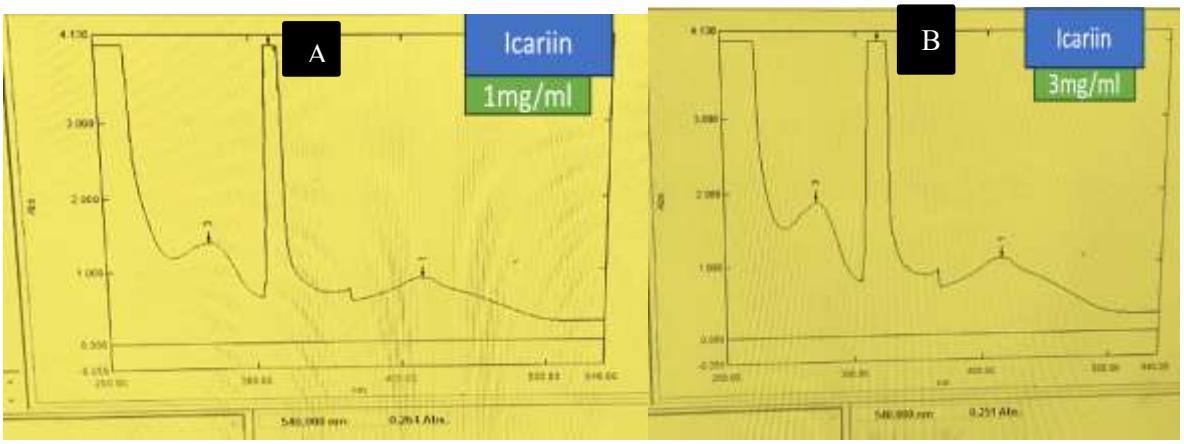

Figure 17:NO SCAVENGING ASSAY, A) IC 1MG/ML, B)IC 3MG/ML

Icariin (1 mg/mL) exhibited major UV–Vis absorption near 270 nm with a secondary peak at 540 nm (0.254 absorbance). Reduced absorbance in the nitric oxide scavenging assay indicated effective radical neutralization, demonstrating antioxidant activity and supporting Icariin's potential as a promising anticancer compound for further therapeutic investigation.

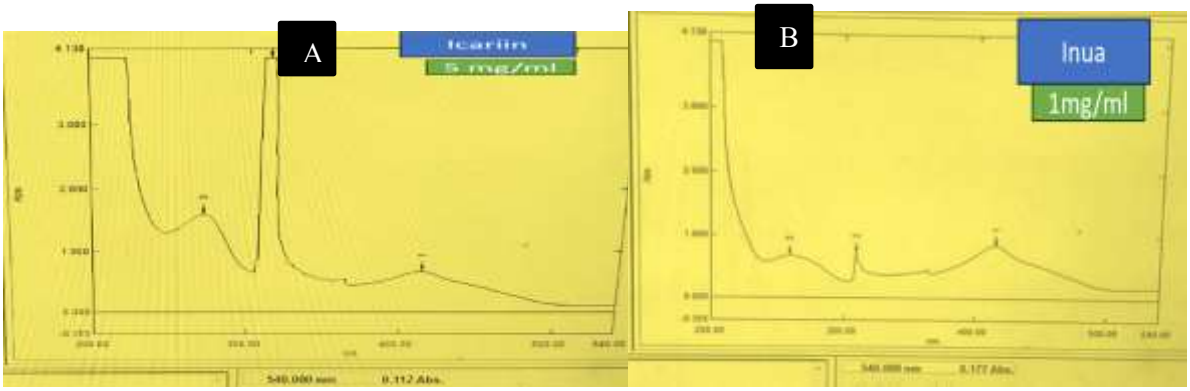

Figure 18:NO SCAVENGING ASSAY, A) IC 5MG/ML, B)InUa 1MG/ML

Icariin (5 mg/mL) exhibited distinct UV–Vis absorption peaks near 270 and 340 nm with an absorbance of 0.112 at 540 nm. Reduced absorbance in the nitric oxide scavenging assay confirmed concentration-dependent antioxidant activity, supporting its ability to reduce oxidative stress and its potential for anticancer drug development.

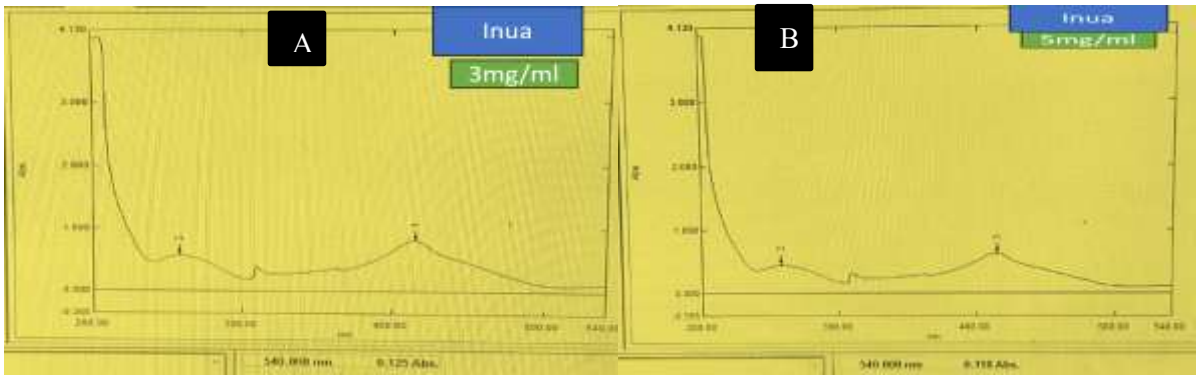

Figure 19:NO SCAVENGING ASSAY, A) InUa 3MG/ML, B)InUa 5MG/ML

InuA (3 mg/mL) exhibited characteristic UV–Vis absorption peaks with an absorbance of 0.125 at 540 nm. Reduced absorbance in the nitric oxide scavenging assay indicated measurable radical neutralization, demonstrating concentration-dependent antioxidant activity and supporting its modest yet promising potential for preliminary anticancer drug screening and evaluation.

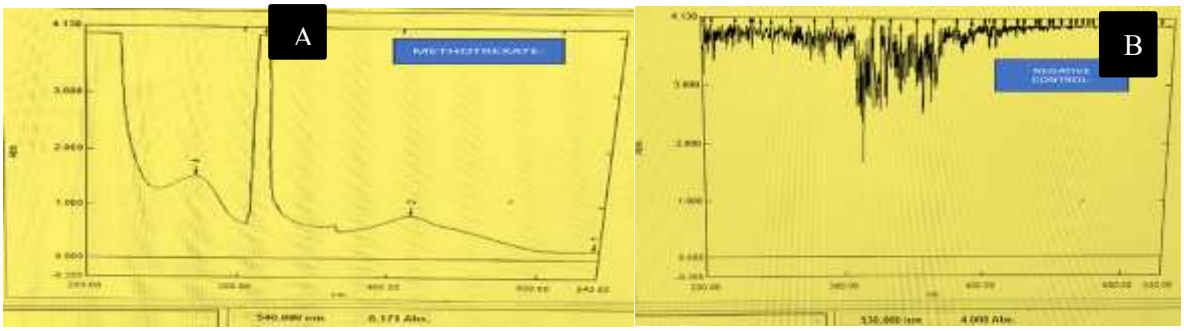

Figure 20:NO SCAVENGING ASSAY, A) MTX, B) NEGATIVE CONTROL

Methotrexate exhibited characteristic UV–Vis absorption peaks near 260 and 370 nm, with an absorbance of 0.171 at 540 nm. Reduced absorbance in the nitric oxide scavenging assay confirmed potent radical neutralization, demonstrating strong antioxidant activity and validating Methotrexate as a reliable positive standard for anticancer drug screening.

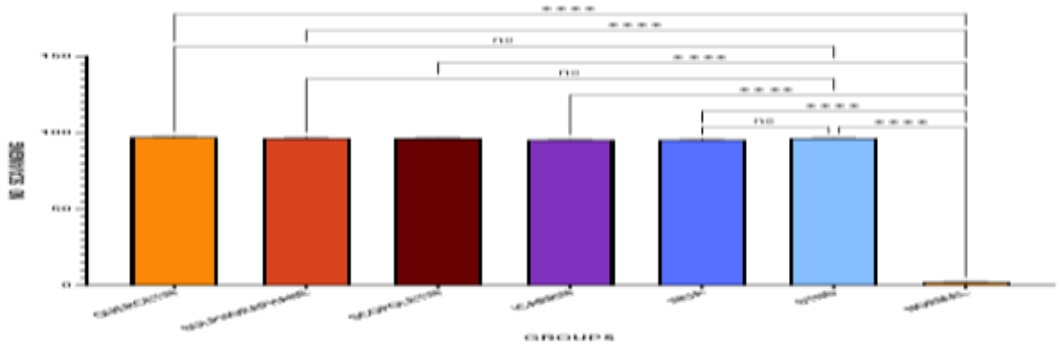

The bar graph demonstrates nitric oxide scavenging activity across experimental groups. The Normal/Negative control showed the lowest activity, whereas Quercetin, Sulforaphane, Scopoletin, Icariin, InuA, and Methotrexate exhibited significantly higher scavenging effects (***p < 0.001–****p < 0.0001). No significant differences occurred among treatment groups, indicating comparable antioxidant and anticancer potential.

3.6.EDTA CHELATING AGENT TEST:

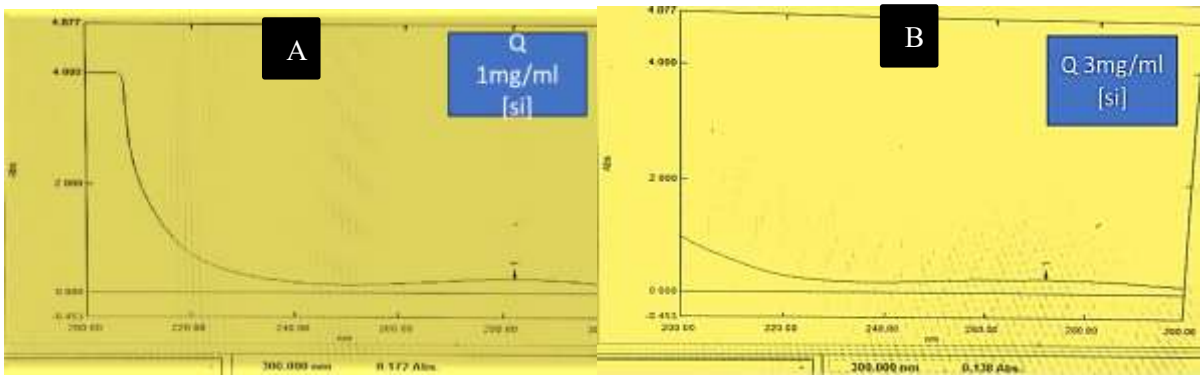

Figure 21:EDTA CHELATING AGENT TEST , A) Q 1MG/ML[SI], B) Q 3MG/ML[SI]

Compound Q showed strong UV absorption with reduced absorbance at 300 nm (0.172 at 1 mg/mL; 0.138 at 3 mg/mL). Lower absorbance in the EDTA metal-chelation assay indicates efficient Fe^{2+} binding, limiting Fenton-mediated hydroxyl radical generation, reducing oxidative stress and DNA damage. Enhanced chelation at higher concentration supports its potential anticancer antioxidant mechanism.

Figure 22:EDTA CHELATING AGENT TEST , A) Q 5MG/ML[SI], B) SU 3MG/ML[HE]

The UV–Visible analysis showed that compound Q (5 mg/mL, SiHa) exhibited very low absorbance at 300 nm (0.055), indicating strong metal-chelating activity, while compound Su (1 mg/mL, HeLa) showed moderate absorbance (0.246), suggesting moderate chelation. By reducing metal-mediated reactive oxygen species generation, both compounds may alleviate oxidative stress and contribute to anticancer activity.

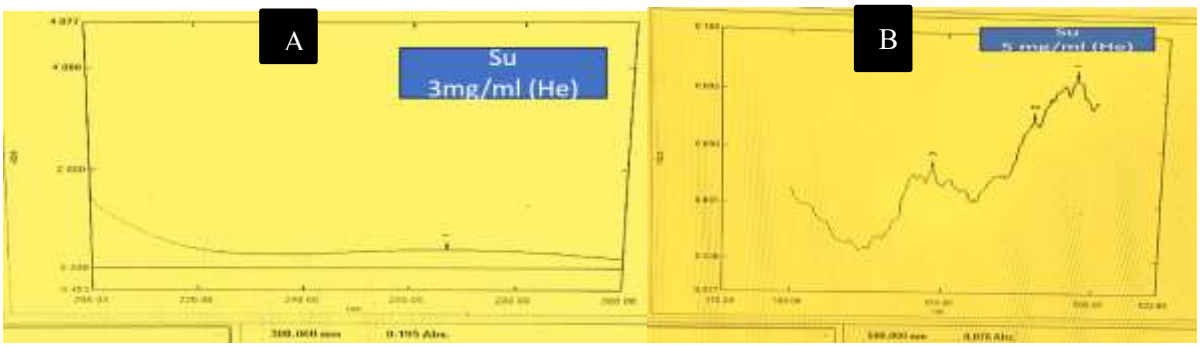

Figure 23:EDTA CHELATING AGENT TEST , A) SU 3MG/ML[HE], B) SU 1MG/ML[HE]

Compound Su demonstrated concentration-dependent metal-chelating activity in HeLa cells. At 3 mg/mL, reduced absorbance at 300 nm (0.195) indicated stronger transition metal ion binding than 1 mg/mL. At 5 mg/mL, minimal absorbance (0.078) reflected enhanced chelation, potentially suppressing reactive oxygen species generation, reducing oxidative stress, and supporting anticancer activity through redox modulation.

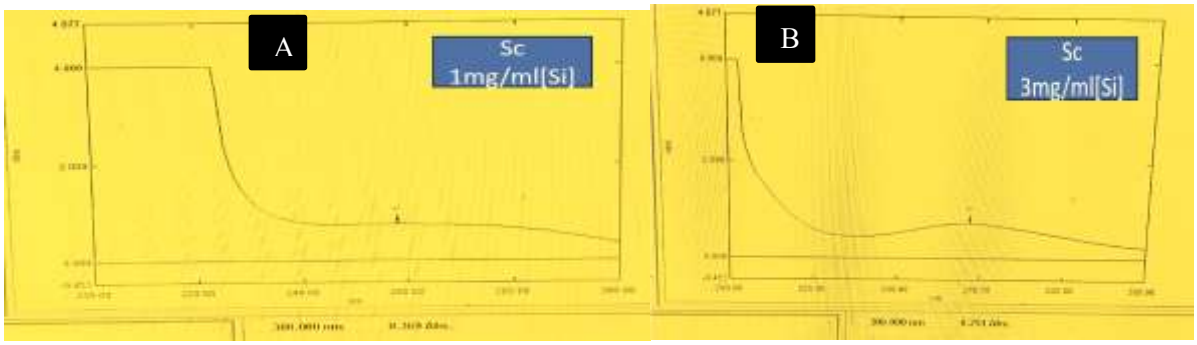

Figure 24:EDTA CHELATING AGENT TEST , A) SC 1MG/ML[SI], B) SC 3MG/ML[SI]

Compound Sc exhibited concentration-dependent metal-chelating activity in SiHa cells. At 1 mg/mL, absorbance at 300 nm was 0.369, while 5 mg/mL reduced it to 0.173, indicating enhanced transition metal ion sequestration. Improved chelation may suppress reactive oxygen species generation, disrupt redox homeostasis, and contribute anti-cancer activity.

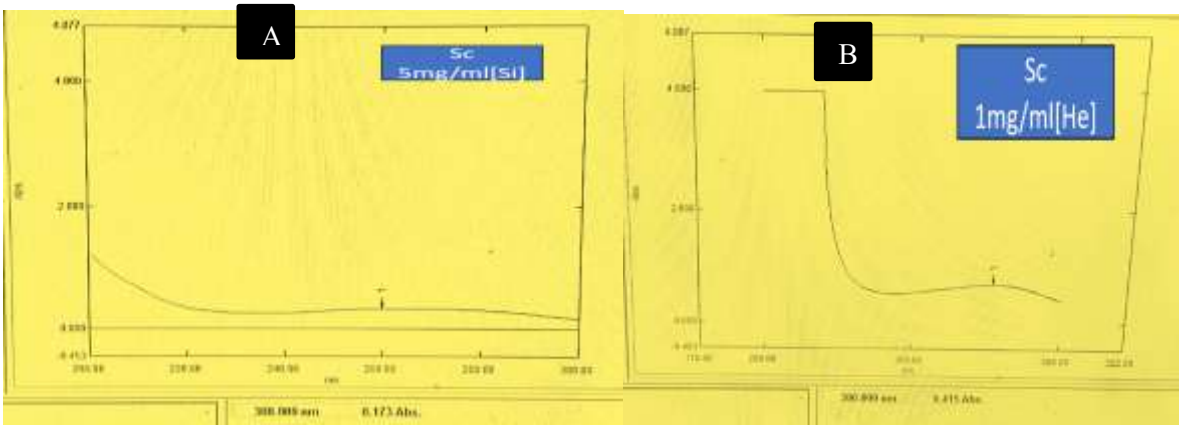

Figure 25:EDTA CHELATING AGENT TEST , A) SC 5MG/ML[SI], B) SC 1MG/ML[HE]

Compound Sc showed effective metal-chelating activity in both cervical cancer models. In SiHa cells (5 mg/mL), absorbance decreased to 0.173 at 300 nm, indicating stronger chelation, whereas in HeLa cells (1 mg/mL), absorbance was 0.415, reflecting moderate activity. Metal ion sequestration may reduce reactive oxygen species generation and support anticancer effects

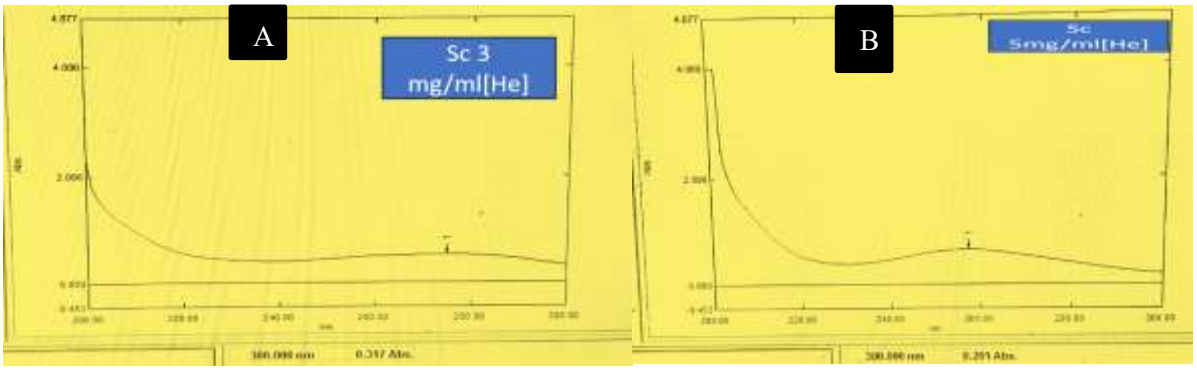

Figure 26:EDTA CHELATING AGENT TEST , A) SC 1MG/ML[HEI], B) SC 3MG/ML[HE]

Compound Sc exhibited dose-dependent metal-chelating activity in HeLa cells. Absorbance decreased from 0.317 at 300 nm (3 mg/mL) to 0.201 (5 mg/mL), indicating enhanced transition metal ion sequestration at higher concentration. Improved chelation may suppress reactive oxygen species generation, disrupt redox homeostasis, and contribute to the compound's potential anticancer efficacy.

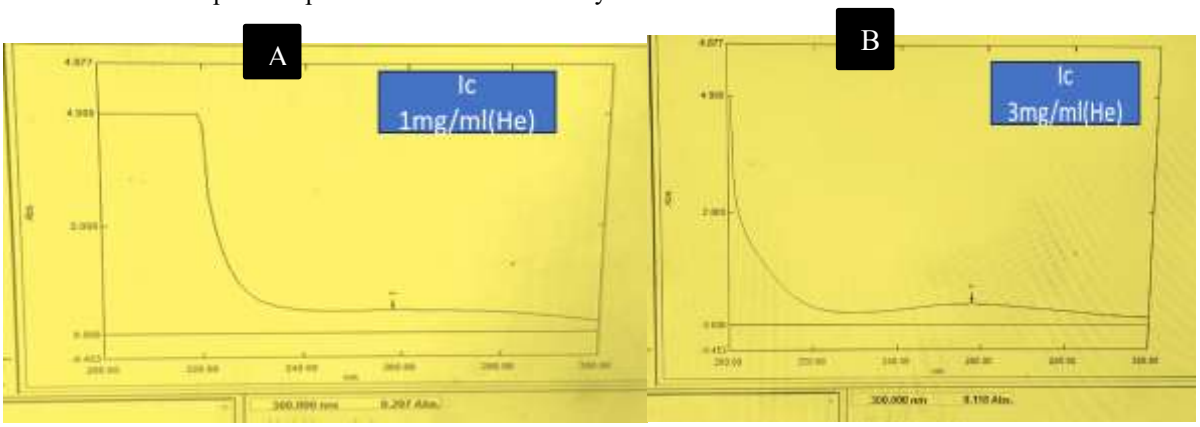

Figure 27:EDTA CHELATING AGENT TEST , A) IC 1MG/ML[HE], B)IC 3MG/ML[HE]

Compound Ic exhibited concentration-dependent metal-chelating activity in HeLa cells. Absorbance at 300 nm decreased from 0.207 (1 mg/mL) to 0.118 (3 mg/mL), indicating enhanced transition metal ion sequestration at higher concentration. Improved chelation may suppress reactive oxygen species generation, disrupt redox homeostasis, and contribute to the compound's potential anticancer activity.

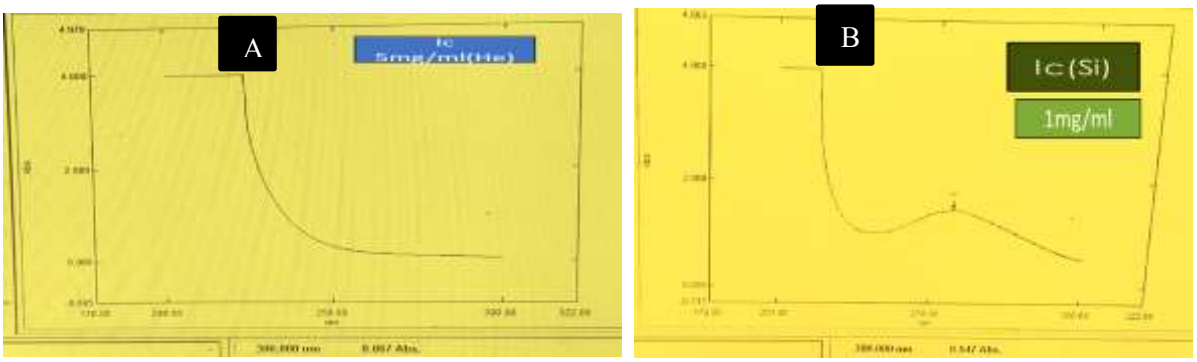

Figure 28:EDTA CHELATING AGENT TEST , A)IC 5MG/ML[HE], B)IC 1MG/ML[SI]

Compound Ic demonstrated effective metal-chelating activity in cervical cancer models. In HeLa cells (5 mg/mL), absorbance decreased to 0.067 at 300 nm, indicating maximum sequestration efficiency. In SiHa cells (1 mg/mL), absorbance was 0.547, confirming chelation capability. Metal ion binding may reduce ROS generation, disrupt redox pathways, and support anticancer potential.

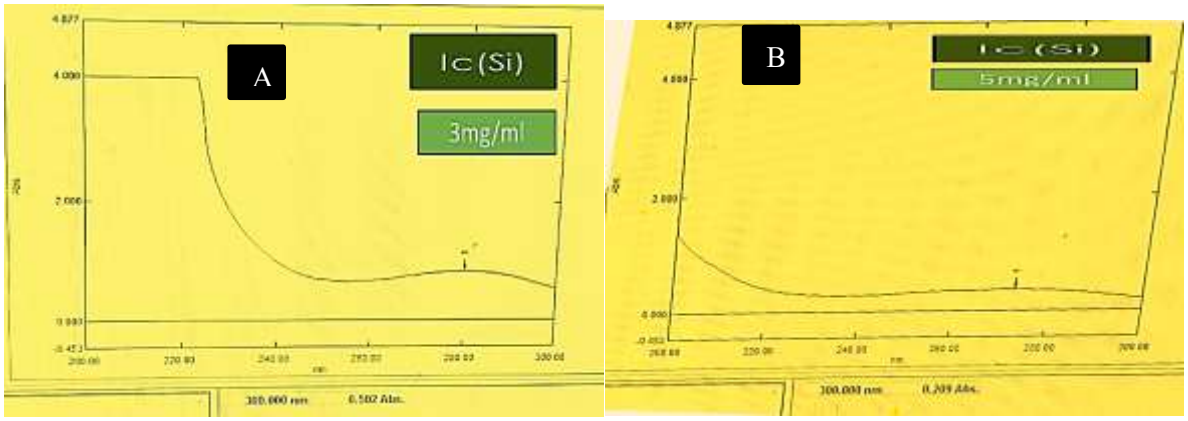

Figure 29:EDTA CHELATING AGENT TEST , A) IC 3MG/ML[SI], B) IC 5MG/ML[SI]

Compound Ic showed concentration-dependent metal-chelating activity in SiHa cells. Absorbance at 300 nm decreased from 0.502 (3 mg/mL) to 0.209 (5 mg/mL), indicating enhanced transition metal ion sequestration. This improved chelation may limit redox cycling, reduce reactive oxygen species generation, disrupt metal-dependent survival pathways, and support the compound's potential anticancer efficacy.

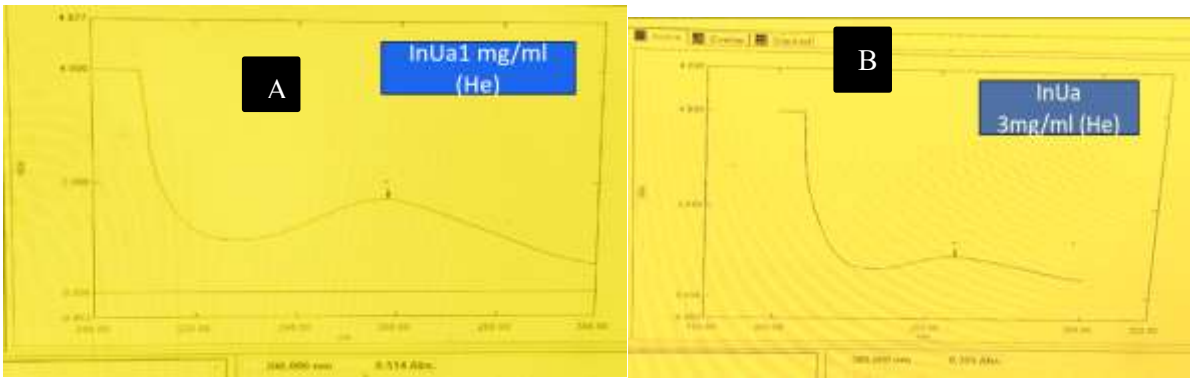

Figure 30:EDTA CHELATING AGENT TEST , A) InUa 1MG/ML[HE], B) iNUa 3MG/ML[HEI]

Compound InUa demonstrated concentration-dependent metal-chelating activity in HeLa cells. Absorbance at 300 nm decreased from 0.514 (1 mg/mL) to 0.395 (3 mg/mL), indicating enhanced transition metal ion sequestration. This activity may suppress redox cycling, reduce reactive oxygen species generation, regulate metal homeostasis, and contribute to the compound's potential anticancer effects.

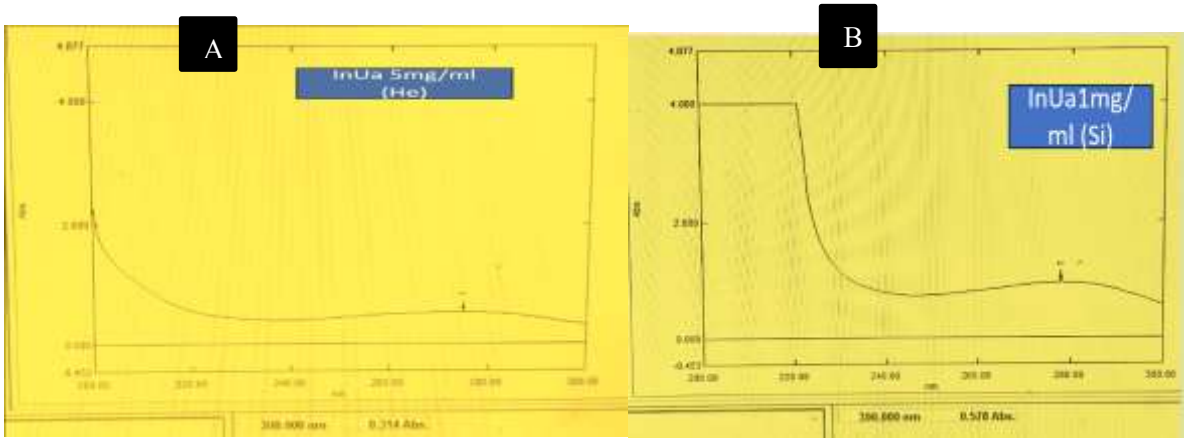

Figure 31:EDTA CHELATING AGENT TEST , A) InuA 5MG/ML[HEI], B)InUa 1MG/ML[SI]

Compound InUa exhibited effective metal-chelating activity in cervical cancer models. In HeLa cells (5 mg/mL), absorbance decreased to 0.314 at 300 nm, indicating maximum sequestration efficiency. In SiHa cells (1 mg/mL), absorbance was 0.578, confirming chelation capability. Metal binding may regulate homeostasis, reduce ROS generation, and support anticancer potential.

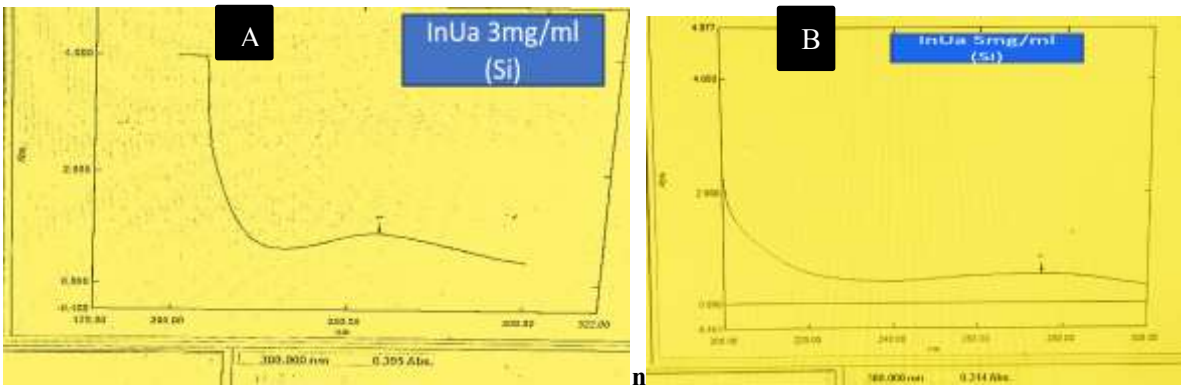

Figure 32:EDTA CHELATING AGENT TEST , A) InUa 3MG/ML[SI], B)Inua 5MG/ML[SI]

Compound InUa (3 mg/mL) showed effective metal-chelating activity in SiHa cells, with absorbance of 0.395 at 300 nm. Its ion-sequestering ability may disrupt redox pathways, reduce oxidative stress, and support anticancer potential.

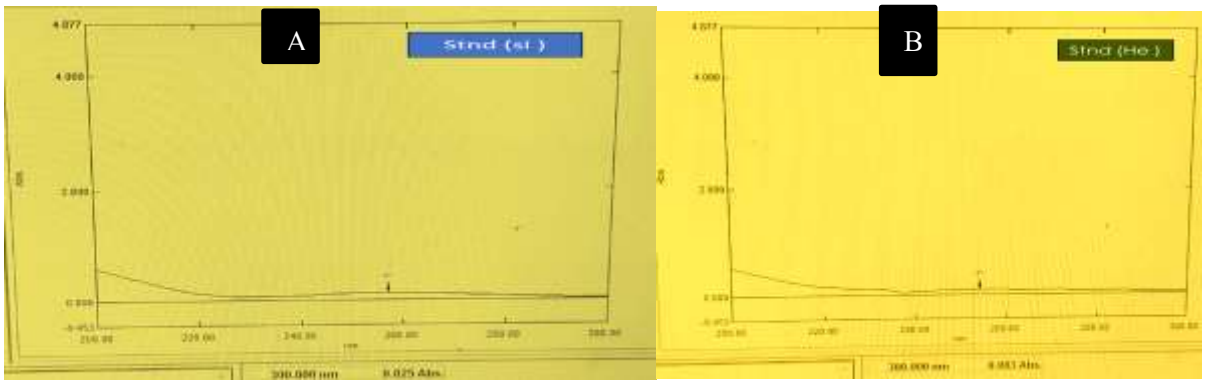

Figure 33:EDTA CHELATING AGENT TEST , A)METHOTREXATE[SI], B) METHOTREXATE[HE]

Compound InUa (5 mg/mL) showed maximum metal sequestration in SiHa cells, with absorbance of 0.314 at 300 nm, indicating strong chelation and redox modulation. Methotrexate (MTX) in HeLa cells showed 0.083 absorbance, serving as a benchmark. Compound Ic (0.067) demonstrated superior activity, followed by Sc and InUa.

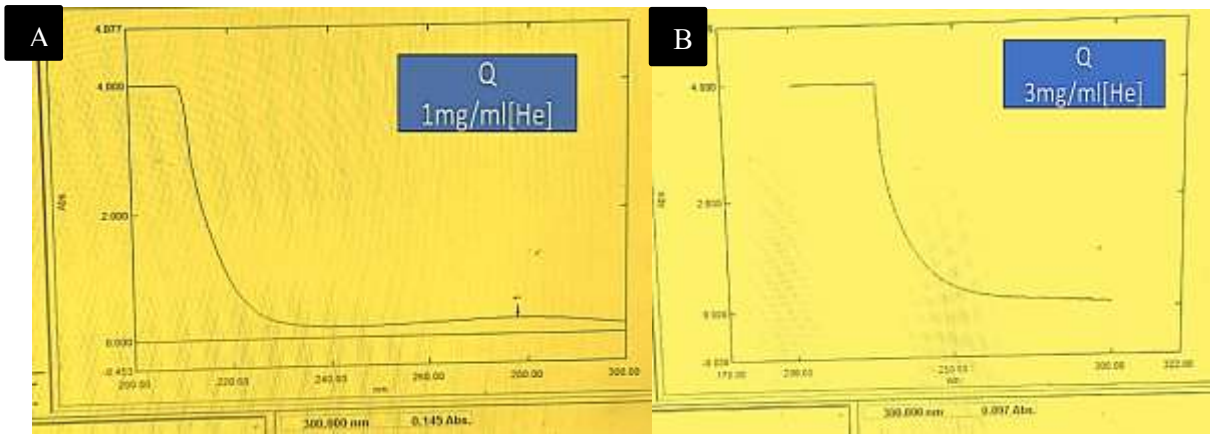

Figure 34:EDTA CHELATING AGENT TEST , A) Q 1MG/ML[HE], B) Q 3MG/ML[HEI]

Compound Q exhibited strong concentration-dependent metal-chelating activity in HeLa cells. Absorbance at 300 nm decreased from 0.145 (1 mg/mL) to 0.097 (3 mg/mL), approaching the Methotrexate benchmark (0.083). This enhanced transition metal sequestration may suppress redox pathways, reduce oxidative stress, and support compound Q as a promising anticancer candidate**.**

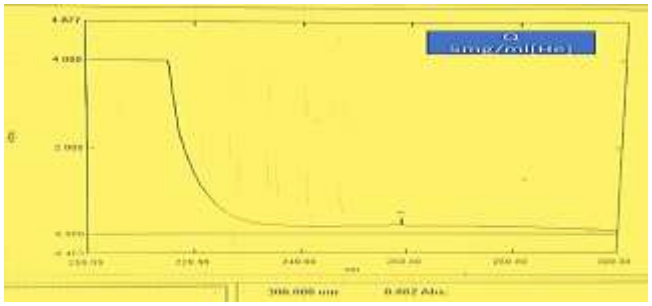

Figure 35:EDTA CHELATING AGENT TEST , Q 5MG/ML[HE]

Compound Q (5 mg/mL) showed maximum metal-chelating efficiency in HeLa cells, with absorbance of 0.082 at 300 nm, comparable to Methotrexate (0.083). This indicates strong ion sequestration, redox modulation, and potential anticancer activity.

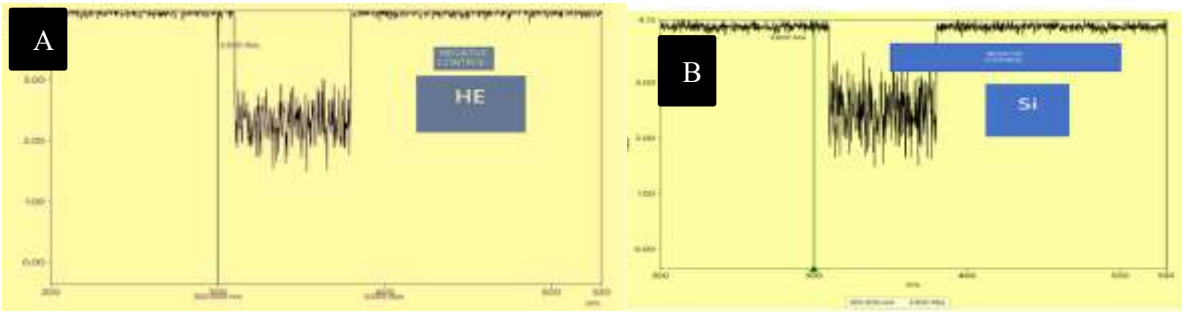

Figure 36:EDTA CHELATING AGENT TEST , A) NEGATIVE CONTROL[HE], B) NEGATIVE CONTROL[SI]

Negative Control (HE) showed maximum absorbance (3.500 at 300 nm) in both HeLa and SiHa models, representing the untreated baseline with active transition metals and oxidative stress. This saturated profile provides a reference for evaluating chelation efficiency. Significant reductions by compounds, such as Compound Q, indicate effective metal sequestration and redox modulation.

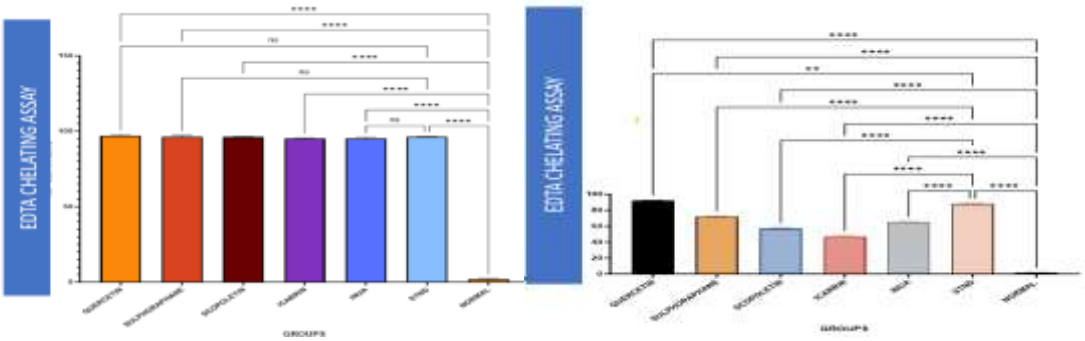

EDTA-like chelating agents demonstrated significant metal-sequestering activity in both HeLa and SiHa cervical cancer models compared with Normal untreated groups. All tested compounds, including Quercetin, Sulforaphane, Scopoletin, Icariin, and InUa, showed highly significant enhancement in chelation capacity ($p < 0.0001$; ****). InUa exhibited comparable efficiency with the standard in HeLa, whereas Quercetin showed the highest SiHa activity, closely approaching the standard. These findings confirm their potential role in regulating redox balance.

3.7. Heat Induced Haemolysis Assay:

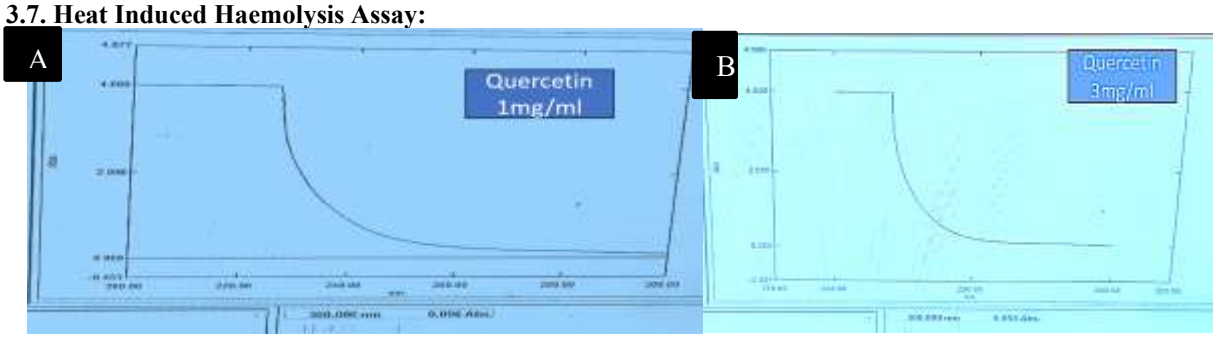

Figure 37:HEAT INDUCED ASSAY , A) Q 1MG/ML[HE], B) Q 3MG/ML

Quercetin showed strong UV absorption with a plateau of 4.000 Abs between 200–230 nm. Absorbance at 300 nm decreased from 0.096 (1 mg/mL) to 0.055 (3 mg/mL), indicating concentration-dependent optical changes. These concentrations demonstrated strong membrane-protective activity, achieving 79.62% and 87.24% inhibition in heat-induced hemolysis assays, supporting its therapeutic potential.

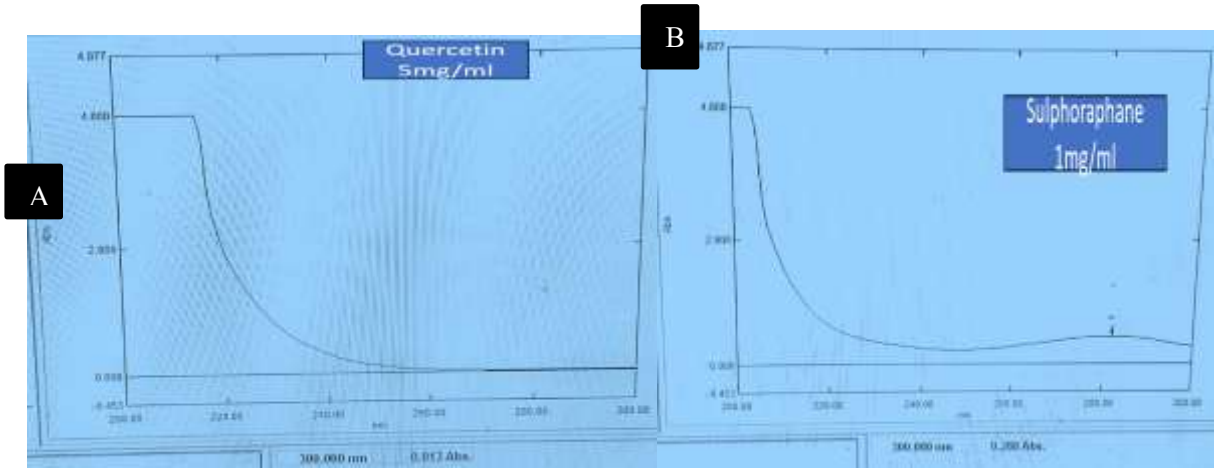

Figure 38:HEAT INDUCED ASSAY , A) Q 5MG/ML, B) SU 1MG/ML

Quercetin (5 mg/mL) showed a saturated UV profile (4.000 Abs, 200–215 nm) with minimal absorbance at 300 nm (0.013), indicating concentration-dependent optical variation and highest hemolysis protection (98.84%). Sulforaphane (1 mg/mL) displayed far-UV saturation with absorbance of 0.288 at 300 nm and moderate hemolysis inhibition (51.76%), confirming biological activity.

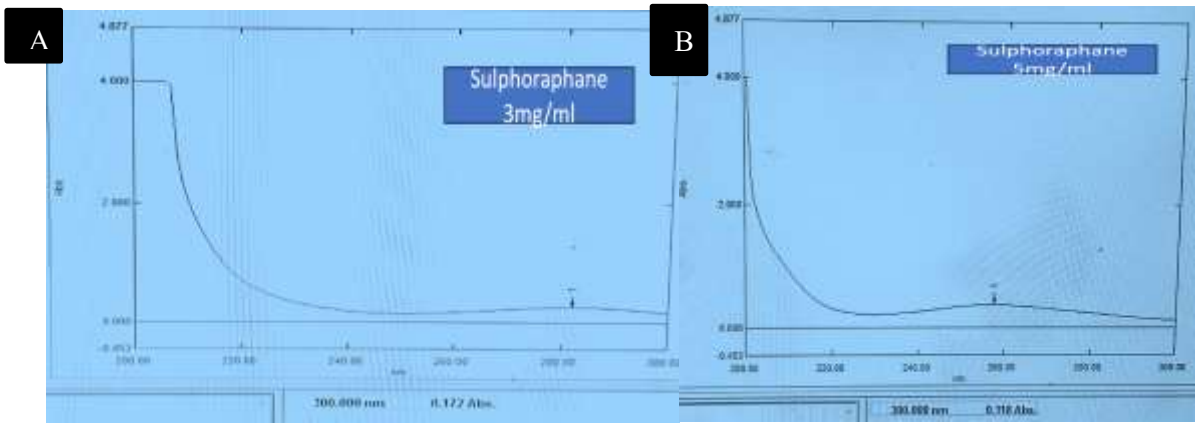

Figure 39: HEAT INDUCED ASSAY , A) SU3MG/ML, B) SU 5MG/ML

Sulforaphane exhibited concentration-dependent UV-Vis changes with far-UV saturation at 4.000 Abs (200–210 nm). Absorbance at 300 nm decreased from 0.288 (1 mg/mL) to 0.172 (3 mg/mL) and 0.118 (5 mg/mL). These concentrations showed enhanced membrane protection, achieving 88.81% and 88.98% hemolysis inhibition, supporting its anticancer potential.

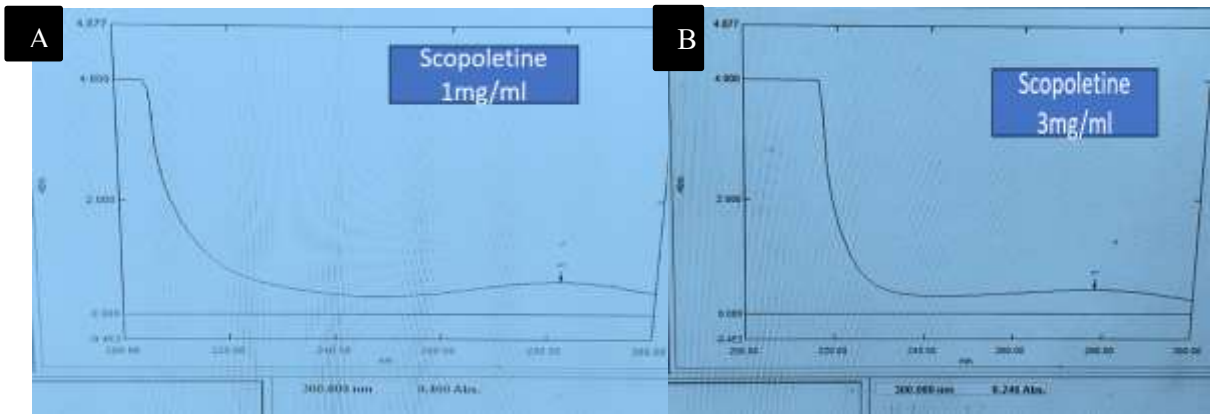

Figure 40:HEAT INDUCED ASSAY , A) SC 1MG/ML, B) SC 3MG/ML

Scopoletin demonstrated concentration-dependent UV-Vis changes and strong membrane stabilization activity. Absorbance at 300 nm decreased from 0.400 (1 mg/mL) to 0.246 (3 mg/mL), indicating enhanced optical response. It protected RBC membranes against thermal damage, achieving 76.02% inhibition at lower concentration and peak efficacy of 95.18%, exceeding the standard (93.74%).

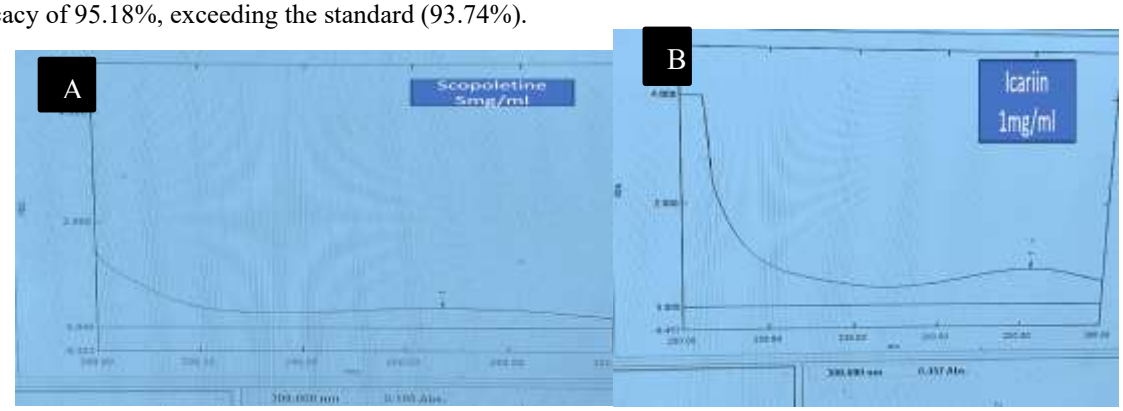

Figure 41:HEAT INDUCED ASSAY , A) SC 5MG/ML, B) IC 1MG/ML

Scopoletin (5 mg/mL) showed maximum membrane protection, with absorbance decreasing to 0.195 at 300 nm and achieving 95.18% hemolysis inhibition, surpassing the standard (93.74%). Icariin (1 mg/mL) exhibited absorbance of 0.457 at 300 nm and 58.21% inhibition, indicating moderate membrane stabilization that may improve with higher

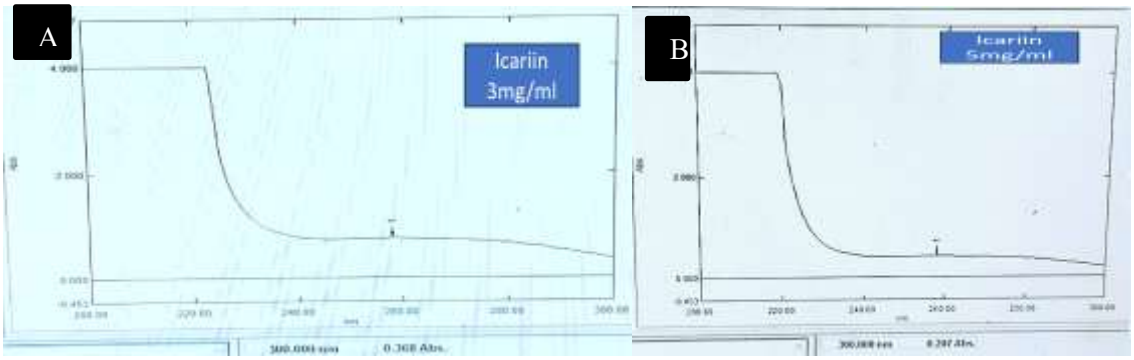

Figure 42:HEAT INDUCED ASSAY , A) IC 3MG/ML, B) IC 5MG/ML

Icariin exhibited concentration-dependent membrane stabilization in the hemolysis assay. Absorbance at 300 nm decreased from 0.457 (1 mg/mL) to 0.368 (3 mg/mL) and 0.207 (5 mg/mL), corresponding to increased RBC protection. Hemolysis inhibition improved from 58.21% to 75.45% and 88.64%, approaching standard efficacy while remaining below Quercetin activity.

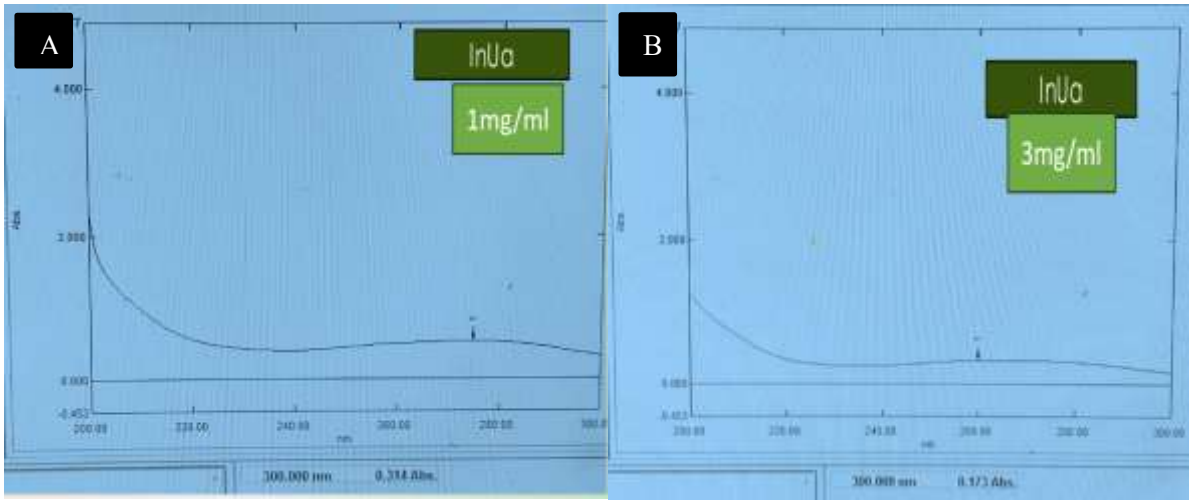

Figure 43:HEAT INDUCED ASSAY , A) INU 1MG/ML, B) INU 3MG/ML

The UV-Vis spectrum for InUa at 1 mg/ml provides the optical baseline for this experimental group in the heat-induced hemolysis assay. The graph displays a rapid exponential decline from the far-UV region, transitioning into a broad, low-intensity absorption peak centered near 275 nm. At the standard 300.00 nm reference point, the sample recorded an absorbance of 0.314 Abs.. Biologically, this concentration achieved a 66.14% inhibition of red blood cell lysis. The UV-Vis spectrum for InUa at 3 mg/ml illustrates a notable optical and biological shift from the lower 1 mg/ml dose. The graph shows a sharp exponential decline from the far-UV region, transitioning into a flattened

absorption curve across the 240–300 nm range. At the 300.00 nm reference point, the sample recorded an absorbance of 0.173 Abs., a significant decrease from the 0.314 Abs. seen at 1 mg/ml. Biologically, this concentration achieved an 86.13% inhibition of red blood cell lysis. This jump from 66.14% confirms that InUa's membrane-stabilizing potency is highly concentration-dependent, providing robust protection against thermal stress .

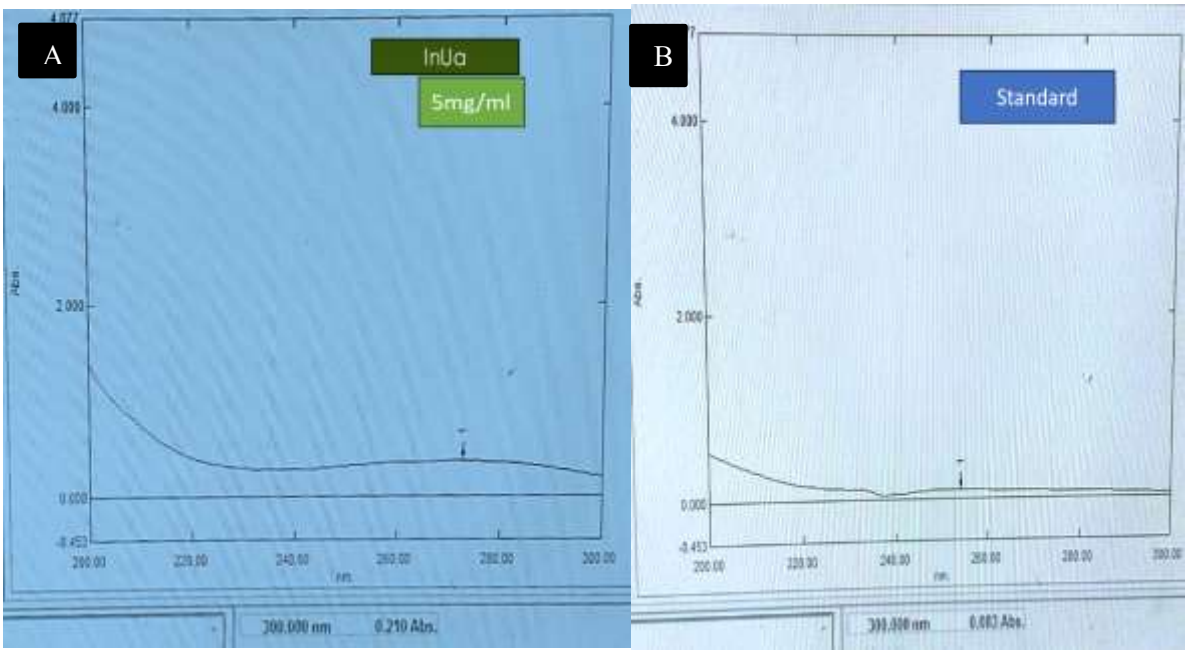

Figure 44:HEAT INDUCED ASSAY , A) INU 5MG/ML, B)STANDARD

The UV-Vis spectrophotometry analysis for InUa at 5 mg/ml represents the peak concentration tested in the heat-induced hemolysis assay. The graph shows a shallow exponential decline from the far-UV region, transitioning into a stabilized baseline with a subtle absorption shoulder centered near 275 nm. At the 300.00 nm reference point, the sample recorded an absorbance of 0.210 Abs.. Biologically, this dose achieved a maximum stabilization rate of 91.13% inhibition of red blood cell lysis. This high efficacy successfully crosses the 90% threshold, indicating that InUa at 5 mg/ml is a potent protector against thermal stress.The UV-Vis spectrum for the Standard group represents the primary reference for maximum stabilization in the heat-induced hemolysis assay. Unlike the drug candidates, the Standard graph lacks a saturation plateau, showing a consistent and highly stable baseline across the entire 200 nm to 300 nm range. At the 300.00 nm reference point, the sample recorded a remarkably low absorbance of 0.083 Abs., which is the lowest value across all tested groups. Biologically, this reflects a high membrane-stabilizing efficacy of 93.74% inhibition.

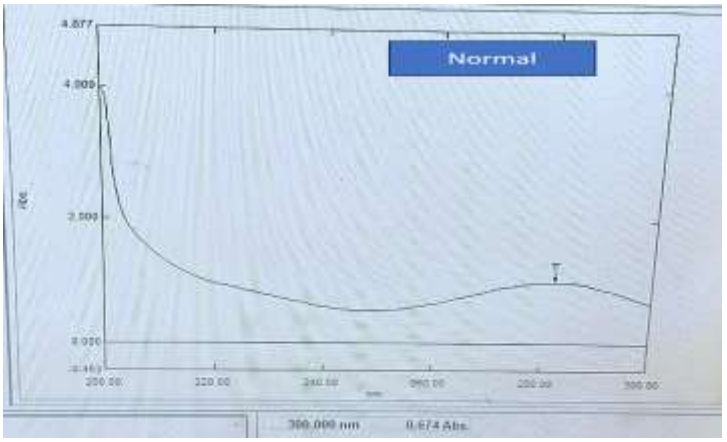

Figure 45:HEAT INDUCED ASSAY , FOR NORMAL GROUP

The UV-Vis spectrum for the Normal (Negative/Untreated) group establishes the baseline for maximum cellular damage in the heat-induced hemolysis assay. The graph shows a steep exponential decline from the far-UV region, transitioning into a prominent absorption peak centered near 285 nm. This peak represents the high concentration of hemoglobin and cellular debris released during uncontrolled thermal lysis. At the 300.00 nm reference point, the sample recorded a high absorbance of 0.674 Abs., the highest value among all primary groups. Biologically, this untreated group represents 0.00% inhibition, serving as the negative control against which the membrane-stabilizing efficacy of all drug candidates is measured.

Conclusions

In this research work we evaluated the anti cancer activity of Quercetin, Sulforaphane, Scopoletine, Icariin, and InuA & these all exhibited significant anticancer potential through cytotoxic, antimicrobial, antioxidant, anti-mitotic, and anti-germination activities. Quercetin showed the highest overall efficacy, while Scopoletine excelled against gram-negative bacteria and InuA displayed strong antioxidant activity, supporting their promising pharmaceutical and anticancer applications.

List of abbreviations:

Abbreviations & Full Forms

UAE – Ultrasonic-Assisted Extraction; UV – Ultraviolet Spectroscopy; HPLC – High-Performance Liquid Chromatography; TLC – Thin Layer Chromatography; NaOH – Sodium Hydroxide; HCl – Hydrochloric Acid; H_2SO_4 – Sulfuric Acid; CH_3OH – Methanol; EtOH – Ethanol; LIB – Libermann's Test; LB – Libermann–Burchard Test; KI – Potassium Iodide; $FeCl_3$ – Ferric Chloride; mg/mL – Milligrams per Milliliter; gm – Grams; mL – Milliliters; Fig. – Figure; INU – Inulin; SULPH – Sulforaphane; QUER – Quercetin; AC – Allium cepa; MTX – Methotrexate; DPPH – 2,2-Diphenyl-1-picrylhydrazyl; µL – Microliter; OD – Optical Density.

Ethics Approval

This study does not involve human participants, human data, or human tissue. It involves Allium cepa, brine shrimp (Artemia salina), and microbial cultures. Therefore, ethics approval and consent to participate are **not applicable**.

Consent to Participate

N/A

Consent for Publication

This manuscript does not contain any individual person's data in any form (including images, videos, or case reports). Therefore, **not applicable**.

Funding

Not applicable.

References

1. World Health Organization. WHO Guideline for Screening and Treatment of Cervical Pre-Cancer Lesions for Cervical Cancer Prevention [Internet]. Geneva: WHO; [cited 2025 Aug 8]. Available from: https://doi.org/10.2471/b09020
2. Biazin H, Mekuria S, Assegid N, Forslund O, Borgfeldt C, Jerkeman M, et al. Sexually transmitted infections and association with high-risk human papillomavirus among Ethiopian women attending cervical cancer screening. 2025. https://doi.org/10.21203/rs.3.rs-5930727/v1
3. Aker SS, Ortaç F. The effect of other high-risk HPV types on cervical intraepithelial neoplasia and cancer. Cervical Cancer. 2020. https://doi.org/10.1136/ijgc-2020-esgo.41
4. Abdel Rahman R, Badawy A, Elsebeiy F, Gouda E. Awareness of women towards risk factors, screening practices and preventive behaviors of cervical cancer. Zagazig Nurs J. 2023;19(1):118–32. https://doi.org/10.21608/znj.2023.296477
5. Unknown Authors. Correlation between high-risk HPV-positive cervical intraepithelial neoplasia (CIN) and vaginal microecological indicators. Adv Clin Med. 2024;14(12):536–44. https://doi.org/10.12677/acm.2024.14123114
6. Zheng L, Lin Y, Wu J, Zheng M. The associations of tobacco use, sexually transmitted infections, HPV vaccination, and screening with the global incidence of cervical cancer: An ecological time series modeling study. Epidemiol Health. 2022;45. https://doi.org/10.4178/epih.e2023005
7. Rajkumari B, Singh WJ, Thounaojam UD, Kasar M, Ranalcis R. Awareness on cervical cancer, its screening, and HPV vaccination among women of reproductive age group (15–49 years) in Manipur. Natl J Community Med. 2025;16(3):271–6. https://doi.org/10.55489/njcm.160320254838
8. Lee DW, Lee KH, Lee JW, Park ST, Park JS, Lee HN. Is neoadjuvant chemotherapy followed by radical surgery more effective than radiation therapy for stage IIB cervical cancer? Int J Gynecol Cancer. 2013;23(7):1303–10. https://doi.org/10.1097/igc.0b013e31829da105
9. Neag MA, Mocan A, Echeverría J, Pop RM, Bocsan CI, Crişan G, et al. Berberis vulgaris fruit: Determination of phenolic compounds in extracts obtained by supercritical CO_2 and Soxhlet methods using HPLC. [Journal information missing]. 2022;15:877–89.
10. Nuralın L, Gürü M. Berberis vulgaris fruit: Determination of phenolic compounds in extracts obtained by supercritical CO_2 and Soxhlet methods using HPLC. Food Anal Methods. 2022;15:877–89. https://doi.org/10.1007/s12161-021-02136-8
11. Dulić M, Ciganović P, Vujić L, Zovko Končić M. Antidiabetic and cosmeceutical potential of common barberry (Berberis vulgaris L.) root bark extracts obtained by optimization of "green" ultrasound-assisted extraction. Molecules. 2019;24(19):3613. https://doi.org/10.3390/molecules24193613

12. Neag MA, Mocan A, Echeverría J. Berberine: Botanical occurrence, traditional uses, extraction methods, and relevance in cardiovascular, metabolic, hepatic, and renal disorders. [Journal information missing].
13. Akansha, Rastogi M, Shaida B. Antioxidant and antibacterial properties of chicory (Cichorium intybus L.) root and leaves extract – An experimental study. J Clin Diagn Res. 2022. https://doi.org/10.7860/JCDR/2022/59187.17042
14. Sigma Aldrich. Mayer's reagent [Internet]. US Pharmacopeia; 2012 [cited 2025 Aug 8]. Available from: https://www.sigmaaldrich.com
15. Pharmacademias. Hager's test [Internet]. [cited 2025 Aug 8]. Available from: https://www.pharmacademias.com
16. Dragendorff's reagent. Historical perspectives and current status of a versatile reagent introduced over 150 years ago at the University of Dorpat, Tartu, Estonia. 2020.
17. Bhandary SK, Kumari SN, Bhat VS, Sharmila KP, Bekal MP. Preliminary phytochemical screening of various extracts of Punica granatum peel, whole fruit, and seeds. Nitte Univ J. 2012 Dec.
18. Patel V, Prajapati M, Modi N. Evaluation of total phenolic and flavonoid content, free radical scavenging activity, and phytochemical screening of fruits of Raphanus caudatus L. Int J Bot Stud. 2021.
19. Vanlalhruaia, Lalbiaknunga J. Detection of cyanogenic glycosides in ethnomedicinal plants of Euphorbiaceae used by tribes in Mizoram, India. J Pharmacogn Phytochem. 2020.
20. Sims IM, Carnachan SM, Bell TJ, Hinkley SFR. Methylation analysis of polysaccharides: Technical advice. Carbohydr Polym. 2018.
21. Islam M, Malakar S, Rao MV, Kumar N, Sahu JK. Recent advancement in ultrasound-assisted novel technologies for the extraction of bioactive compounds from herbal plants: a review. **Food Sci Biotechnol.** 2023;32(13):1763-1782. doi:10.1007/s10068-023-01346-6.
22. Sahu AK, Singh VK, Singh DK, et al. Design of experiments for optimizing ultrasound-assisted extraction of bioactive compounds from plant-based sources. **Foods.** 2023;12(24):4445. doi:10.3390/foods12244445.
23. Chua LS, Chong KF, Sarmidi MR, et al. A review of ultrasound-assisted extraction for plant bioactive compounds: phenolics, flavonoids, thymols, saponins and proteins. **Food Res Int.** 2022;157:111268. doi:10.1016/j.foodres.2022.111268.
24. Azmir J, Zaidul ISM, Rahman MM, et al. Techniques for extraction of bioactive compounds from plant materials: a review. **J Food Eng.** 2022;321:110986. doi:10.1016/j.jfoodeng.2022.110986.
25. Zhang QW, Lin LG, Ye WC. Techniques for extraction and isolation of natural products: a comprehensive review. **Chin Med.** 2023;18:12. doi:10.1186/s13020-023-00724-6.
26. Tille PM. **Bailey & Scott's Diagnostic Microbiology.** 15th ed. St. Louis: Elsevier; 2022.
27. Cappuccino JG, Welsh CT. **Microbiology: A Laboratory Manual.** 12th ed. Boston: Pearson; 2023.
28. Leboffe MJ, Pierce BE. **A Photographic Atlas for the Microbiology Laboratory.** 5th ed. Englewood: Morton Publishing Company; 2021.
29. Balouiri M, Sadiki M, Ibnsouda SK. Methods for in vitro evaluating antimicrobial activity: a review. **J Pharm Anal.** 2016;6(2):71-79. doi:10.1016/j.jpha.2015.11.005.
30. Wiegand I, Hilpert K, Hancock REW. Agar and broth dilution methods to determine the minimal inhibitory concentration (MIC) of antimicrobial substances. **Nat Protoc.** 2008;3(2):163-175. doi:10.1038/nprot.2007.521.
31. Eloff JN. A sensitive and quick microplate method to determine the minimal inhibitory concentration of plant extracts for bacteria. **Planta Med.** 1998;64(8):711-713. doi:10.1055/s-2006-957563.
32. Andrews JM. Determination of minimum inhibitory concentrations. **J Antimicrob Chemother.** 2001;48(Suppl 1):5-16. doi:10.1093/jac/48.suppl_1.5.
33. Blois MS. Antioxidant determinations by the use of a stable free radical. **Nature.** 1958;181:1199-1200. doi:10.1038/1811199a0.
34. Brand-Williams W, Cuvelier ME, Berset C. Use of a free radical method to evaluate antioxidant activity. **LWT Food Sci Technol.** 1995;28(1):25-30. doi:10.1016/S0023-6438(95)80008-5.
35. Molyneux P. The use of the stable free radical diphenylpicrylhydrazyl (DPPH) for estimating antioxidant activity. **Songklanakarin J Sci Technol.** 2004;26(2):211-219.
36. Makkar HPS, Siddhuraju P, Becker K. **Plant Secondary Metabolites.** Totowa: Humana Press; 2007.
37. Raskin I, Ripoll C. Can an apple a day keep the doctor away? Current research on the health benefits of apples. **Trends Plant Sci.** 2004;9(11):538-543. doi:10.1016/j.tplants.2004.09.004.
38. AOSA. **Seedling Evaluation Handbook.** Contribution No. 35. Ithaca: Association of Official Seed Analysts; 2002.
39. Bewley JD. Seed germination and dormancy. **Plant Cell.** 1997;9(7):1055-1066. doi:10.1105/tpc.9.7.1055.
40. ISTA. **International Rules for Seed Testing.** Bassersdorf: International Seed Testing Association; 2023.
41. Mizuno K, Mizuno M, Hattori K, et al. Protein degradation technologies as therapeutic strategies for cancer treatment: current progress and future perspectives. **Cancer Sci.** 2023;114(7):2581-2593. doi:10.1111/cas.15789.
42. Goldberg AL. Protein degradation and protection against misfolded or damaged proteins. **Nature.** 2003;426(6968):895-899. doi:10.1038/nature02263.
43. Kumari S, Badana AK, Malla R. Protein denaturation and stabilization assays for evaluating bioactive compounds: methods and applications in drug discovery. **J Pharm Biomed Anal.** 2021;193:113738. doi:10.1016/j.jpba.2020.113738.
44. Sreejayan N, Rao MNA. Nitric oxide scavenging by curcuminoids. **J Pharm Pharmacol.** 1997;49(1):105-107. doi:10.1111/j.2042-7158.1997.tb06761.x.

45. Marcocci L, Maguire JJ, Droy-Lefaix MT, Packer L. The nitric oxide-scavenging properties of Ginkgo biloba extract EGb 761. **Biochem Biophys Res Commun.** 1994;201(2):748-755. doi:10.1006/bbrc.1994.1769.
46. Green LC, Wagner DA, Glogowski J, Skipper PL, Wishnok JS, Tannenbaum SR. Analysis of nitrate, nitrite, and [15N]nitrate in biological fluids. **Anal Biochem.** 1982;126(1):131-138. doi:10.1016/0003-2697(82)90118-X.
47. Kumar S, Sharma S, Vasudeva N. Review on antioxidant and nitric oxide scavenging activity of natural compounds: methods and applications. **Phytochem Anal.** 2021;32(4):534-548.
48. Tsikas D. Analysis of nitrite and nitrate in biological fluids by assays based on the Griess reaction: appraisal of the Griess reaction. **J Chromatogr B Analyt Technol Biomed Life Sci.** 2007;851(1-2):51-70. doi:10.1016/j.jchromb.2006.07.054.
49. Decker EA, Welch B. Role of ferritin as a lipid oxidation catalyst in muscle food. **J Agric Food Chem.** 1990;38(3):674-677. doi:10.1021/jf00093a019.
50. Dinis TCP, Madeira VMC, Almeida LM. Action of phenolic derivatives (acetaminophen, salicylate, and 5-aminosalicylate) as inhibitors of membrane lipid peroxidation and as peroxyl radical scavengers. **Arch Biochem Biophys.** 1994;315(1):161-169. doi:10.1006/abbi.1994.1485.
51. Santos-Buelga C, Scalbert A. Proanthocyanidins and tannin-like compounds—nature, occurrence, dietary intake and effects on nutrition and health. **J Sci Food Agric.** 2000;80(7):1094-1117. doi:10.1002/(SICI)1097-0010(20000515)80:7<1094::AID-JSFA569>3.0.CO;2-1.
52. Gülçin İ. Antioxidant activity of food constituents: an overview. **Arch Toxicol.** 2012;86(3):345-391. doi:10.1007/s00204-011-0779-2.
53. Shinde UA, Phadke AS, Nair AM, Mungantiwar AA, Dikshit VJ, Saraf MN. Membrane stabilizing activity—A possible mechanism of action for the anti-inflammatory activity of Cedrus deodara wood oil. **Fitoterapia.** 1999;70(3):251-257. doi:10.1016/S0367-326X(99)00030-1.
54. Oyedapo OO, Akinpelu BA, Akinwunmi KF, Adeyinka MO, Sipeolu FO. Red blood cell membrane stabilizing potentials of extracts of Lantana camara and Tithonia diversifolia. **Int J Plant Physiol Biochem.** 2010;2(4):46-51.
55. Anosike CA, Obidoa O, Ezeanyika LUS. Membrane stabilization as a mechanism of the anti-inflammatory activity of methanol extract of Gardenia ternifolia leaves. **Int J Biomed Res.** 2012;3(1):9-14.
56. Mizushima Y, Kobayashi M. Interaction of anti-inflammatory drugs with serum proteins, especially with some biologically active proteins. **J Pharm Pharmacol.** 1968;20(3):169-173. doi:10.1111/j.2042-7158.1968.tb09718.x.
57. Williams LAD, O'Connar A, Latore L, et al. The in vitro anti-denaturation effects induced by natural products and their potential as anti-inflammatory agents. **West Indian Med J.** 2008;57(4):327-331.